

STELLAR RADIAL VELOCITIES IN THE OLD OPEN CLUSTER M67 (NGC 2682) I. MEMBERSHIPS, BINARIES, AND KINEMATICS *

AARON M. GELLER^{†,‡}

Center for Interdisciplinary Exploration and Research in Astrophysics (CIERA) and Department of Physics & Astronomy, Northwestern University, Evanston, IL 60201, USA,

Department of Astronomy and Astrophysics, University of Chicago, 5640 S. Ellis Avenue, Chicago, IL 60637, USA; a-geller@northwestern.edu

DAVID W. LATHAM

Harvard-Smithsonian Center for Astrophysics, 60 Garden Street, Cambridge, MA 02138, USA; dlatham@cfa.harvard.edu

ROBERT D. MATHIEU[†]

Department of Astronomy, University of Wisconsin - Madison, WI 53706, USA; mathieu@astro.wisc.edu

ABSTRACT

We present results from 13776 radial-velocity measurements of 1278 candidate members of the old (4 Gyr) open cluster M67 (NGC 2682). The measurements are the results of a long-term survey that includes data from seven telescopes with observations for some stars spanning over 40 years. For narrow-lined stars, radial velocities are measured with precisions ranging from about 0.1 to 0.8 km s⁻¹. The combined stellar sample reaches to the brightest giants in the cluster down to about 4 magnitudes below the main-sequence turnoff ($V = 16.5$), covering a mass range of about 1.34 M_⊙ to 0.76 M_⊙. Spatially, the sample extends to a radius of 30 arcminutes (7.4 pc in projection at a distant of 850 pc or 6-7 core radii). We find M67 to have a mean radial velocity of +33.64 km s⁻¹ (with an internal precision of ±0.03 km s⁻¹) well separated from the mean velocity of the field. For stars with ≥3 measurements, we derive radial-velocity membership probabilities and identify radial-velocity variables, finding 562 cluster members, 142 of which show significant radial-velocity variability. We use these cluster members to construct a color-magnitude diagram and identify a rich sample of stars that lie far from the standard single star isochrone, including the well-known blue stragglers, sub-subgiants and yellow giants. These exotic stars have a binary frequency of (at least) 80%, more than three times that detected for stars in the remainder of the sample. We confirm that the cluster is mass segregated, finding the binaries to be more centrally concentrated than the single stars in our sample at the 99.8% confidence level (and at the 98.7% confidence level when only considering main-sequence stars). The blue stragglers are centrally concentrated as compared to the solar-type main-sequence single stars in the cluster at the 99.7% confidence level. Accounting for measurement precision, we derive a radial-velocity dispersion in M67 of 0.80 ± 0.04 km s⁻¹ for our sample of single main-sequence stars, subgiants and giants with $V \leq 15.5$. When corrected for undetected binaries, this sample yields a true radial-velocity dispersion of 0.59^{+0.07}_{-0.06} km s⁻¹. The radial distribution of the velocity dispersion is consistent with an isothermal distribution within our stellar sample. Using the cluster radial-velocity dispersion, we estimate a virial mass for the cluster of 2100⁺⁶¹⁰₋₅₅₀ M_⊙.

open clusters and associations: individual (NGC 2682) – binaries: spectroscopic – methods: observational – techniques: spectroscopic – blue stragglers – stars: kinematics and dynamics

1. INTRODUCTION

M67 (NGC 2682) is one of the few old and rich open clusters in our Galaxy, and therefore is central to our understanding of stellar evolution, stellar dynamics and star cluster evolution. M67 is located at $\alpha = 8^h 51^m 23^s.3$, $\delta = +11^\circ 49' 02''$ (J2000). With an age of about 4 Gyr (Nissen et al. 1987; Montgomery et al. 1993; Demarque et al. 1992; Carraro et al. 1994; Fan et al. 1996; VandenBerg & Stetson 2004; Balaguer-Núñez et al. 2007) and a half-mass relaxation time of about 100 Myr (Mathieu & Latham

1986), M67 is a highly dynamically evolved system. Importantly, M67 is relatively nearby, with recent distance measurements ranging from between about 800 pc to 900 pc (Janes 1985; Nissen et al. 1987; Montgomery et al. 1993; Carraro et al. 1994; Fan et al. 1996; Grocholski & Sarajedini 2003; Sandquist 2004; Balaguer-Núñez et al. 2007; Pasquini et al. 2008; Sarajedini et al. 2009), and has low extinction, with recent $E(B - V)$ determinations between 0.015 and 0.056 (Janes & Smith 1984; Burstein et al. 1986; Montgomery et al. 1993; Carraro et al. 1994; Fan et al. 1996; Taylor 2007). Furthermore, most studies agree that M67 has a roughly solar metallicity, with recent [Fe/H] values ranging from -0.10 to +0.05 (Janes & Smith 1984; Burstein et al. 1986; Nissen et al. 1987; Montgomery et al. 1993; Fan et al. 1996; Randich et al. 2006; Balaguer-Núñez et al. 2007;

*WIYN OPEN CLUSTER STUDY. LXVII.

[†]Visiting Astronomer, Kitt Peak National Observatory, National Optical Astronomy Observatory, which is operated by the Association of Universities for Research in Astronomy (AURA) under cooperative agreement with the National Science Foundation.

[‡]NSF Astronomy and Astrophysics Postdoctoral Fellow

Taylor 2007; Friel et al. 2010; Pancino et al. 2010; Jacobson et al. 2011). Thus M67 provides a large sample of solar-type dwarf and evolved stars that are easily accessible to a variety of ground-based (and space-based) observations.

Indeed, M67 has been extensively studied through photometry from X-rays to near-IR (Belloni et al. 1998; Vandenberg & Stetson 2004; Landsman et al. 1998; Nissen et al. 1987; Montgomery et al. 1993; Fan et al. 1996; Balaguer-Núñez et al. 2007; Yadav et al. 2008; Sarajedini et al. 2009), including several time-series optical photometric surveys (Gilliland et al. 1991, 1993; van den Berg et al. 2002; Stassun et al. 2002; Sandquist & Shetrone 2003b; Bruntt et al. 2007; Pribulla et al. 2008; Yakut et al. 2009). These surveys have revealed many intriguing stars, some of which lie far from the standard single-star evolutionary sequence in a color-magnitude diagram (CMD).

In order to interpret these observations, kinematic membership probabilities are paramount. There have been a number of proper-motion surveys of M67 (Sanders 1977; Girard et al. 1989; Zhao et al. 1993; Yadav et al. 2008, and see also Loktin 2005), to various limiting magnitudes and spatial extents. There have also been a few radial-velocity (RV) surveys (Mathieu et al. 1986, 1990; Milone 1992; Milone & Latham 1994; Yadav et al. 2008; Pasquini et al. 2011). Surveys such as these have confirmed the kinematic cluster memberships of a rich population of blue straggler stars (BSS; residing blueward of and generally brighter than the main-sequence turnoff), yellow giants (residing between the BSS region and the normal giant sequence), and “sub-subgiants” (residing to the red of the main sequence but fainter than the subgiant branch, and also known as “red stragglers”), among the kinematic cluster members (see Figure 8 and Section 6.2).

Numerous theoretical efforts have aimed to explain the origins of these exotic stars through studies of the dynamical evolution of M67 (e.g. Leonard & Linnell 1992; Leonard 1996; Hurley et al. 2005). These studies show that close stellar encounters, and particularly those involving binary stars, may be relatively frequent in M67 and can lead to the creation of exotic stars similar to those observed in the true cluster. Furthermore, these models emphasize the importance of binaries to the dynamical evolution of the cluster.

To date, the published results of the binary population in M67 has been limited. The largest study of binaries in M67 is that of Mathieu et al. (1990), who observed a sample of bright ($V < 12.8$) proper-motion members, and present orbits for 22 spectroscopic binaries. We have continued to monitor these and other stars in M67 in order to extend our sample of detected binaries (and those with orbital solutions) to longer orbital periods, fainter magnitudes and a larger distance from the cluster center. A progress report summarizing the characteristics of 85 spectroscopic binaries was presented at the General Assembly of the IAU in Prague (Latham 2007).

Here we present results from our ongoing RV survey of the cluster. To date we have obtained 13776 RV measurements¹ of 1278 stars in M67 with $8 \leq V \leq 16.5$

(about $1.34 M_{\odot}$ to $0.76 M_{\odot}$) and extending spatially to 30 arcmin in radius from the cluster center (7.4 pc in projection at a distance of 850 pc, or approximately 6 to 7 core radii).² Our stellar sample spans from the brightest stars in the cluster down to 4 magnitudes below the main-sequence turnoff. Also for reference, Fan et al. (1996) find a half-mass radius for stars in our observed magnitude range in M67 of about 10 to 11 arcmin. Tidal radius estimates for the cluster range from 50 arcmin to 100 arcmin (Keenan et al. 1973; Piskunov et al. 2008; Davenport & Sandquist 2010).

In Section 2, we define our stellar sample in detail, and in Sections 3 and 4 we describe our observations and the completeness of our data. In short, our observations are nearly complete within our “primary sample” of stars with $V \leq 15.5$ and within 30 arcmin from the cluster center. Within this primary sample, we have at least one RV measurement for all but one star and at least 3 RV measurements for all but four stars (two of which are rapid rotators). None of these four stars with < 3 RV measurements in our primary sample are proper-motion members; moreover, we have at least three RV measurements for all proper-motion members in our primary stellar sample. Our time baseline of observations for some stars reaches to over 40 years.

Throughout this paper, we use a cutoff of at least 3 RV measurements before attempting to derive RV membership probabilities and variability statistics. Extensive Monte Carlo analyses by Mathieu (1983) and Geller & Mathieu (2012) indicate that 3 RV measurements over the course of at least one year is sufficient to detect nearly all binaries with orbital periods of less than 10^3 days. With our observations, we can detect binaries with significantly longer periods, out to $\sim 10^4$ days. The detection of binaries is particularly important for determining reliable RV membership probabilities. In general, binaries without RV orbital solutions do not yield precise RV membership probabilities, due to their unknown center-of-mass (γ -) RVs. We discuss our identification of binaries and cluster members in Section 5, and we present a summary table of our results for each observed star in Table 4.

Finally, in Section 6 we use our cluster members to investigate the CMD (cleaned from field star contamination), a few stars of note, the projected radial distribution of different cluster populations, and the velocity dispersion and virial mass of the cluster. Then in Section 7 we summarize our results.

2. STELLAR SAMPLE

Our RV survey of M67 began as part of the dissertation work of Mathieu (1983), taking advantage of the CfA Digital Speedometers (DS; Latham 1985, 1992). Three nearly identical instruments were used, initially on the MMT and 1.5-m Tillinghast Reflector at the Fred

therefore count the number of spectra that result in at least one RV measurement). We do not add to our count additional RVs from, for instance, the secondaries of SB2s.

² Zhao et al. (1996) derive a core radius for M67 of 5.2 arcmin. Bonatto & Bica (2003) use 2MASS data to derive a core radius for M67 of 4.86 arcmin. Davenport & Sandquist (2010) revised this result by reanalyzing 2MASS data, and find a core radius of 4.12 arcmin (but a much larger core radius of 8.24 ± 0.60 arcmin when using the fainter stars in their SDSS sample). Therefore our sample extends to between approximately 6 and 7 core radii.

¹ Throughout this paper, when quoting numbers of RV measurements, we provide the number of RVs from the primary stars (and

TABLE 1
TIME SPAN OF DATA FROM EACH TELESCOPE

Telescope	HJD _{start}	HJD _{end}	Days	N_{stars}	N_{obs}
Palomar Hale 5m	2440952	2445297	4345	112	367
Tillinghast 1.5m + DS	2444184	2454958	10774	357	4670
CORAVEL	2444340	2446413	2073	5	92
MMT + DS	2445337	2450830	5493	376	1889
Wyeth 1.5m + DS	2445722	2453433	7711	34	332
WIYN + Hydra	2453386	2456709	3323	1163	5753
Tillinghast 1.5m + TRES	2455143	2456801	1658	111	672

Lawrence Whipple Observatory on Mount Hopkins, Arizona, and then later on the 1.5-m Wyeth Reflector at the Oak Ridge Observatory in the Town of Harvard, Massachusetts. Subsequently the M67 target samples were expanded several times. RV measurements from other programs were integrated into the database, and our observational facilities were extended to include Hydra at the WIYN Observatory³ and TRES on the Tillinghast Reflector. In Table 1 we list the different telescopes and instruments used for this project, along with the dates, number of stars observed and number of observations from each telescope. For the record, here we briefly review the history of what now constitutes more than 40 years of observations, and end by defining the M67 stellar sample that comprises the foundation of this paper.

2.1. CfA

After exploratory observations of a few stars, the initial CfA sample was defined in 1982 as all stars with Sanders (1977) proper-motion membership probabilities greater than 50%, $V < 12.8$ and $(B - V) > 0.40$. This sample comprised the top of the main sequence, subgiants and the giant branch. (The Sanders 1977 study covers a square of approximately 80 arcmin on a side, centered on the cluster.) A study to monitor the RVs of the 13 classical blue stragglers in M67 was being pursued independently (Latham & Milone 1996), and the relevant results from that survey are included in this paper as a convenience to the reader. Also, a subset of 28 giants and subgiants were observed more intensively from Spring 1982 to Spring 1983.

By Spring 1988 the target sample expanded substantially to include all Sanders (1977) members to $V = 14$, and all members in the cluster core (radius < 10 arcmin) to $V = 16$ (only observable with the MMT), totaling 432 stars. The last surviving CfA Digital Speedometer, on the 1.5-m Tillinghast Reflector, was retired in the summer of 2009. Over the following five observing seasons the new Tillinghast Reflector Echelle Spectrograph (TRES) was used to continue the RV observations of targets (mostly binaries) from both the CfA and the WIYN samples. Whenever the observations accumulating for a target suggested that the velocity was not constant, additional observations were scheduled at a frequency designed to reveal its orbital parameters. For some systems the CfA observations span almost 35 years.

Importantly, Roger Griffin and James Gunn also had a RV program for M67 from 1971 to 1982 at the

Palomar Hale 5m telescope, which they supplemented with contemporaneous observations obtained with the CORAVEL instrument at Haute Provence for five of the binaries. Their target sample was very similar to our initial sample, and the combination of the two data sets to expand the time baseline was a natural and straightforward step. The integration of the Palomar and CORAVEL data with the CfA data is discussed in detail in Mathieu et al. (1986), where the entirety of the Palomar data as well as the CfA data to that date are presented, and in Mathieu et al. (1990).

Hereinafter, we will refer to the target stars and the measurements taken at all telescope/instrument pairs except WIYN/Hydra as the CfA sample and data. As of February 2015, there are 447 stars in the CfA sample. The radius – V -magnitude distribution of the stars observed by these telescopes is shown in Figure 1 (top), and the middle and bottom panels of the same figure present the chronology of observations graphically.

2.2. WIYN Stellar Sample

As evident in Figure 1, the CfA sample is not comprehensive in radius for the fainter stars in the sample. Furthermore, the Sanders (1977) proper-motion study was progressively more incomplete and less precise with increasing magnitude. The Hydra Multi-Object Spectrograph (MOS) on the WIYN 3.5m telescope, combined with modern target lists, has been able to provide a complete magnitude and spatially limited sample, as described here.

WIYN observations of M67 began on January 15, 2005 as part of the WIYN Open Cluster Study (WOCS; Mathieu 2000). The current WIYN target list contains all stars with $10 \leq V \leq 16.5$ and within 30 arcminutes in radius from the cluster center. We drew our sample (including astrometric positions) from the 2MASS catalog, supplemented with photometry from Montgomery et al. (1993). The Hydra MOS on WIYN has a 1° field of view, which sets the radial extent of the WIYN survey.

We can derive reliable RVs with our WIYN observing setup for stars with $(B - V)_0 > 0.4$. (Rapid rotation and a diminished number of absorption features often hinders our ability to derive precise RVs for earlier-type stars.) The only stars in M67 that are bluer than this limit and bright enough to be within our sample are BSS. Because of their scientific interest, we included these stars in the WIYN stellar sample. In total there are 1278 stars within the WIYN stellar sample; 382 of these stars are also in the CfA stellar sample. We show the radius – V -magnitude distribution for stars observed at WIYN in the top panel of Figure 2.

³ The WIYN Observatory is a joint facility of the University of Wisconsin-Madison, Indiana University, the National Optical Astronomy Observatory and the University of Missouri.

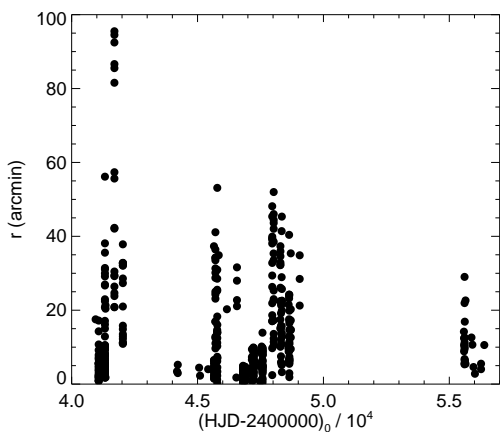
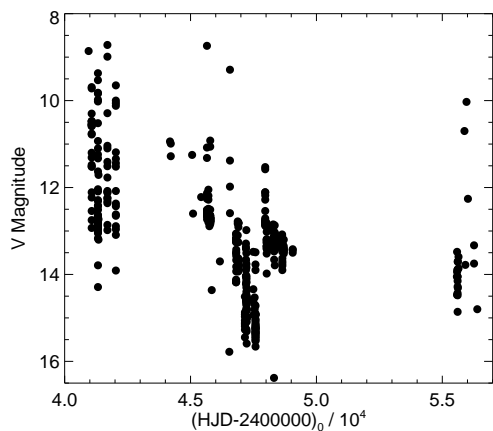
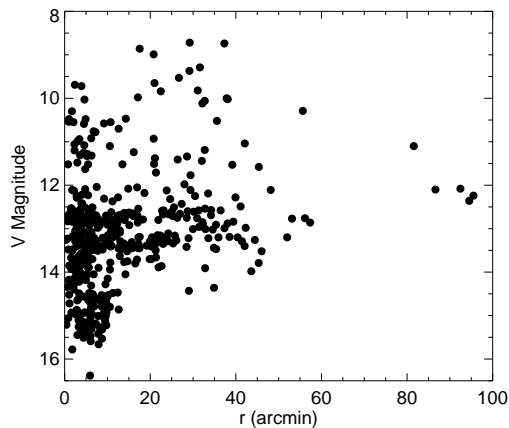


FIG. 1.— The CfA stellar sample, showing (top) V magnitude as a function of radius from the cluster center, and the chronology of the sample, with V magnitude (middle) and radial distance from the cluster center (bottom) plotted as functions of the HJD of the first observation, respectively, for all CfA observed stars.

As seen in Figure 2 (middle), the V magnitude range of the stars observed at WIYN has evolved with time. Initially we chose to make use of WIYN’s advantage at faint magnitudes and prioritized stars from $12.5 < V < 16.5$. (The Hydra MOS has a dynamic range limit of 4 mag.) Later, to improve the completeness of our observations within the combined WIYN and CfA sample, we extended our WIYN sample to include all stars within a 30 arcminute radius from the cluster center and with

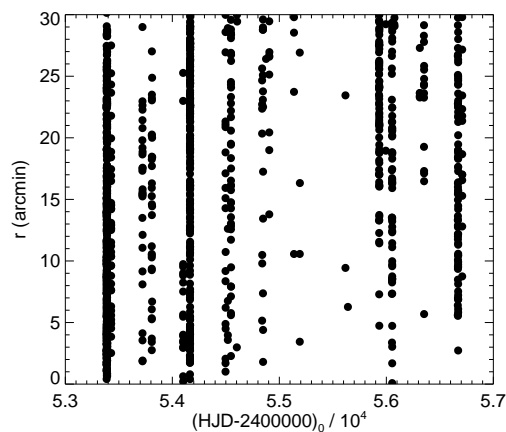
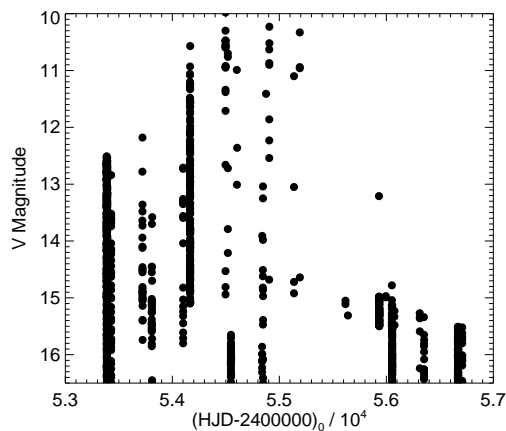
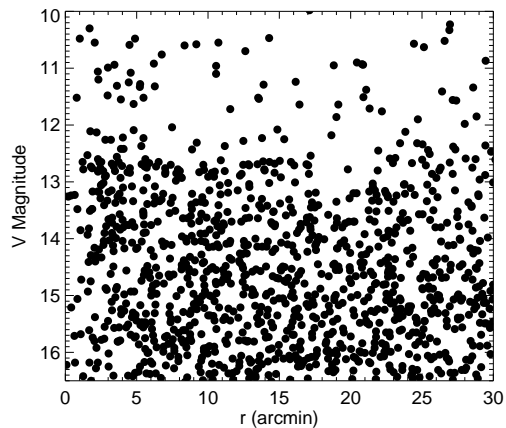


FIG. 2.— The WIYN stellar sample, showing (top) V magnitude as a function of radius from the cluster center, and the chronology of the sample, with V magnitude (middle) and radial distance from the cluster center (bottom) plotted as functions of the HJD of the first observation, respectively, for all WIYN observed stars.

$10 \leq V \leq 16.5$. For a few epochs, we focused exclusively on the brighter stars in our list in order to build this complete sample.

We also note that we removed from our sample the few high-proper-motion stars in the M67 field whose coordinates have changed significantly during the course of our survey, as these stars are certainly not cluster members.

3. OBSERVATIONS

Details about the telescopes, observing procedures, and data reductions of spectra obtained with the CfA Digital Speedometers can be found in Latham (1985, 1992). The corresponding information for spectra obtained with Hydra at the WIYN Observatory can be found in Geller et al. (2008, 2010) and Hole et al. (2009). We describe briefly here the TRES instrument and observations.

TRES is a stabilized fiber-fed echelle spectrograph with a CCD detector and resolution of 44,000. Procedures were adopted to ensure that the RVs from TRES could be adjusted to the native velocity system of the CfA Digital Speedometers. Although TRES delivers wavelength coverage from 390 to 900 nm, only the order centered on the Mg b features was used to derive RVs in order to match the spectral region used by the CfA Digital Speedometers, using the same library of synthetic template spectra for the correlation analysis. To establish the zero point offset between the TRES and CfA Digital Speedometer RVs, observations of the afternoon blue sky and of selected IAU standards were obtained on most nights. There were several modifications to TRES during the first years of its operation, and corresponding zero-point shifts as large as 0.1 km s^{-1} were measured. Since March 2012 the TRES zeropoint has been stable at the level of about 0.01 km s^{-1} .

The TRES velocities are all (initially) shifted by the gravitational redshift of the Sun and blueshift of the Earth, because the library of templates does not include either of those effects. Therefore the derived stellar velocities are all redshifted by the net amount, nominally $+0.62 \text{ km s}^{-1}$, which we subtract out. Furthermore, the native CfA Digital Speedometer velocity system is shifted by -0.14 km s^{-1} compared to the IAU system (Stefanik et al. 1999)⁴. The actual correction to get the TRES velocities onto the native CfA system is observed to be -0.75 km s^{-1} , very close to $-0.62 - 0.14 = -0.76 \text{ km s}^{-1}$. We report TRES velocities on this native CfA system.

We do not apply any shift to the WIYN RVs, and, as noted in Section 4, we do not detect any significant zero-point shift between the WIYN RVs and the native CfA system. Therefore by construction, all RVs reported here, as well as the mean RV of the cluster, are on the native CfA system.

3.1. Radial-Velocity Precision

In order to detect binaries (and higher-order systems), we require multiple observations at multiple epochs with known RV precisions. Our sample contains observations of mainly narrow-lined stars within a modest magnitude range, but taken at multiple different telescopes with different instruments. Therefore to facilitate our subsequent analysis of binarity (Section 5.1), we estimate single-measurement precision values for RVs derived from each respective telescope.

The majority of the CfA measurements come from the MMT and the Tillinghast Reflector (both using the Digital Speedometers). We follow the same procedure as Geller et al. (2008) to empirically determine the typical

single-measurement precision for observations made at these two telescopes and at the WIYN Observatory with Hydra. Specifically we fit a χ^2 distribution of two degrees of freedom to the distribution of standard deviations of the first three RV measurements for each single-lined star in these samples, respectively. The results for all stars observed ≥ 3 times at these telescopes are shown in Figures 3. The dashed lines in each panel of Figure 3 show the best fitting χ^2 distribution functions, respectively, which yield typical single-measurement precision values of 0.8 km s^{-1} for RVs from the Tillinghast Reflector + DS, 0.7 km s^{-1} for RVs from the MMT, and 0.5 km s^{-1} for RV from WIYN. These single-measurement RV precision values for the CfA telescopes are in good agreement with those found by Mathieu et al. (1986), and also agree with the value found by Hole et al. (2009) for observations of NGC 6819 taken at the MMT and the Tillinghast Reflector with the same instrumental setup. Likewise, the single-measurement RV precision for observations at WIYN found here is similar to that found for the narrow-lined stars in NGC 188, NGC 6819 and M35 observed with this same setup (Geller et al. 2008, 2010; Hole et al. 2009).

For these three telescopes (WIYN, MMT and Tillinghast + DS), we also have sufficient data to characterize our RV precision as a function of V magnitude (which, in general, correlates with the signal-to-noise of the measurement for a given integration time). As also found by Geller et al. (2008) and Mathieu et al. (1986) the single-measurement RV precision degrades towards fainter magnitudes. In Figure 4 we show the single-measurement precision values resulting from χ^2 distribution fits to observations from these three telescopes in bins of the stars' V magnitudes. The lines show linear fits to these data. To avoid unrealistic precision values, we impose a precision floor at the values in the bin containing the brightest stars, specifically at 0.4 km s^{-1} for WIYN RVs and 0.6 km s^{-1} for MMT and Tillinghast + DS RVs. We then use these fit lines to determine our single-measurement precision values for stars observed at these telescopes (given their respective V magnitudes) in later analyses.

We also note that observations of the few rapidly rotating stars in our sample have poorer precision (see Geller et al. 2010 for a detailed discussion of the effects of stellar rotation on the WIYN RV precision). For these few stars, we do not attempt to derive single-measurement RV precisions.

We lack sufficient observations on the remaining telescopes to reliably utilize the χ^2 distribution fitting technique. For the Palomar Hale 5m RVs, the typical standard deviation of the measurements of a given star is 0.3 km s^{-1} (Mathieu et al. 1986); we use this value as our single-measurement RV precision for stars observed at Palomar. For observations from the Wyeth 1.5m, there are only 12 stars with at least three RV measurements, and a third of these stars are in binaries (with orbital solutions). The mean of the standard deviations of the first three RVs for the remaining eight stars is 0.4 km s^{-1} , and we take this as an estimate of the single-measurement RV precision for observations from the Wyeth. CORAVEL and TRES observations were primarily of binaries. For CORAVEL RVs, we estimate the RV precision based on the $(O - C)$ residuals from the orbital fits in Mathieu et al. (1990), and find a typi-

⁴ Note that the offset of the CfA Digital Speedometer native velocity system reported in that paper has the wrong sign.

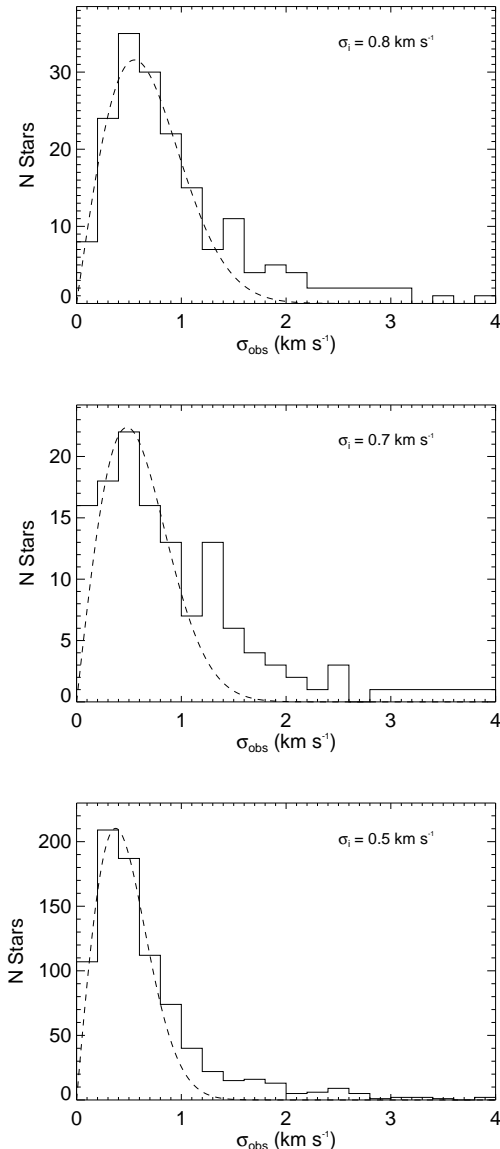


FIG. 3.— Histograms of the RV standard deviations of the first three RV measurements for all stars observed ≥ 3 times at the Tillinghast Reflector + DS (top), MMT (middle) and the WIYN (bottom) telescopes. Also shown in the dashed line in each panel is the best fitting χ^2 function for each distribution. The fits yield a single-measurement precision of 0.8 km s^{-1} for Tillinghast + DS RVs, 0.7 km s^{-1} for MMT RVs and 0.5 km s^{-1} for WIYN RVs. See also Figure 4 for an analysis of the RV precision as a function of the stars’ V magnitudes.

cal precision of 0.5 km s^{-1} .

The correction of the TRES velocities for shifts in the instrumental zero-point from month to month and year to year is now reliable at the level of 0.02 km s^{-1} or better (e.g. see Quinn et al. 2014), much better than the precision achieved for most of our TRES spectra of M67 stars due to SNR limitations set by photon noise. Nevertheless, most of our TRES observations of slowly-rotating single-lined stars in M67 do yield a velocity precision on the order of 0.1 (or perhaps 0.2) km s^{-1} . We assume a single-measurement RV precision of 0.1 km s^{-1} for TRES observations of narrow-lined stars in the following anal-

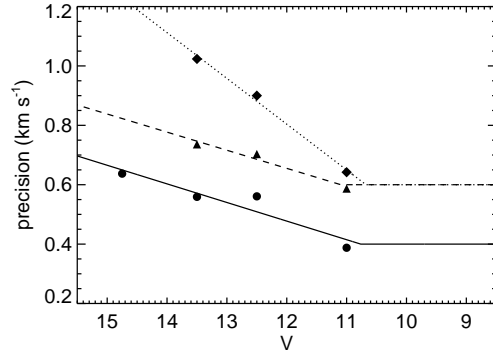


FIG. 4.— Single-measurement RV precision as a function of V magnitude for stars observed at the WIYN telescope (circles and solid line), MMT (triangles and dashed line) and the Tillinghast Reflector + DS (diamonds and dotted line). The points are placed at the centers of bins in V magnitude (with edges at $V = 15.5, 14, 13, 12, 10$), and show results from our fits to χ^2 distributions within these respective bins for each telescope. The lines show linear fits to these data, with a floor of 0.4 km s^{-1} for WIYN RVs and 0.6 km s^{-1} for both the MMT and Tillinghast + DS RVs.

yses.

TRES observations of rapidly-rotating stars have proven to be much more precise than the results for the same stars observed with the CfA Digital Speedometers. We attribute this to the higher SNR and better wavelength coverage provided by TRES. In particular, TRES has allowed us to derive reliable RVs for two of the rapidly rotating BSS in M67 that eluded success with our other facilities.

The long tails in the distributions extending beyond the best fitting curves shown in Figure 3 are populated by binary (and higher-order) systems. Moreover, because the standard deviation of the RVs from a binary should be significantly larger than the single-measurement RV precision, we use the results of this analysis to identify binaries in our sample. We discuss our criteria for identifying binaries in Section 5.1.

4. THE COMBINED CFA AND WIYN DATA SET

The Palomar velocities were adjusted to the native CfA velocity system as described in Mathieu et al. (1986). Here we check for a possible zero-point offset between the WIYN and CfA data by comparing the mean RVs for non-RV variable stars in both samples. Specifically we select only those stars that have three or more observations in both samples, with $P(\chi^2) > 0.01$ and $e/i < 3$ (we discuss the derivation of these quantities in Section 5.1). There are 95 such stars in our sample, and for each of these stars we calculate the mean RV from each sample. The mean RVs for stars in the CfA sample that have observations at multiple telescopes are weighted by the respective precision values discussed above. We then calculate the star-by-star difference in the mean RVs, defined as $RV_{\text{CfA}} - RV_{\text{WIYN}}$, and find a mean difference of 0.008 km s^{-1} , with a standard error of the mean of 0.06 km s^{-1} . As this difference is well below the RV precision of any telescope used here (and less than the magnitude of the offset of the native CfA system from the IAU system, as discussed in Section 3), we conclude that there is no significant zero-point offset at this level

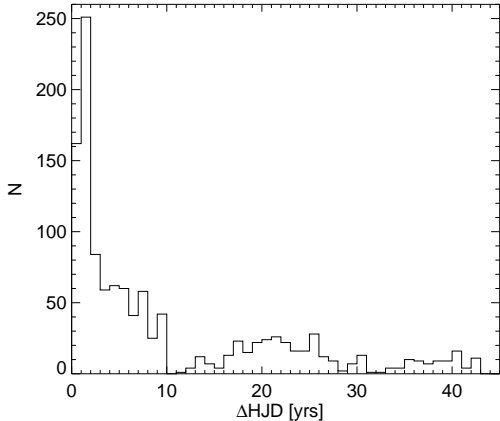


FIG. 5.— Histogram of the maximum time span of RV measurements for stars in our M67 sample that have at least 2 observations.

between the WIYN and CfA RVs.

We therefore proceed in combining the two data sets without modification, and use this combined data set for the following analyses. In total there are 8023 RVs of 455 stars from the CfA and 5753 RVs of 1163 stars from WIYN for a total of 13776 RVs of 1278 stars in M67.

In Figure 5 we plot a histogram of the maximum time span of RV measurements for the stars in our M67 sample (with at least 2 observations). For some stars, our observations span >40 years, and about one third of the stars in our sample have observations spanning at least 10 years. This long time baseline facilitates the detection of long-period binaries in our sample. Again, we discuss our binary detection method in Section 5.1.

4.1. Completeness of Spectroscopic Observations

We define a “primary stellar sample” which extends from the brightest stars in the cluster to $V \leq 15.5$ and out to a 30 arcmin radius from the cluster center. In total, there are 903 stars in our primary sample. We have at least one RV measurement for 902 of these stars, and ≥ 3 RV measurements for 899 of these stars. Moreover, there is only one star without any RV measurements; 2038 (S2312)⁵ is the second brightest star in our primary sample, is brighter than our WIYN sample, and is a Sanders (1977) proper-motion non-member. The other three stars with < 3 RV measurements are 1016 (S1306), 7033 (S1594), 7054 (F1295). 1016 is the brightest star in our sample and is a proper-motion non-member from three sources. We have two observations of 1016 that are outside of the cluster RV distribution. We have observed 7033 and 7054 multiple times, and they both appear to be rapid rotators. We have been unable to derive reliable RVs from the majority of these measurements. 7033 has one proper-motion membership probability (from Sanders 1977) of 0%. 7054 has no proper-motion measurements. Our one tentative RV measurement of 7054 is outside of the cluster RV distribution, but is uncertain due to the rotation. In short, we have RVs for all likely cluster members within our complete sample.

⁵ See Section 5 for an explanation of our nomenclature for our IDs and cross-reference IDs.

Figure 6 shows the percentage of stars with RV measurements in our stellar sample as functions of V magnitude, $(B-V)$ color and distance from the cluster center. There is no significant trend in our completeness within the primary sample with magnitude, color or radius. We show our completeness for stars with $15.5 \leq V \leq 16.5$ in the left panel of Figure 6 within the gray region. There are 418 stars within this magnitude range that are within 30 arcmin from the cluster center. We have at least one RV measurement for 295 (71%) of these stars, and ≥ 3 RV measurements for 182 (44%) of these stars. As shown in Figure 1, the CfA sample also contains observations of stars located at >30 arcmin from the cluster center. We do not include these stars in our primary sample used in the subsequent analyses, but we include all observed stars in our RV summary table (Table 4, presented in Section 5).

5. RESULTS

In the following sections we analyze the RV measurements of each star in our stellar sample. We first assess the RV variability of each star and then the membership probability. We use these quantities to classify stars with ≥ 3 observations as cluster members or non-members, and RV variables (e.g., binaries) or non-variables (e.g., single stars). We present the results of this analysis in Table 4, where we provide the WOCS ID (ID_W)⁶, a cross-reference ID (ID_X)⁷, the J2000 right ascension (RA) and declination (Dec), the V magnitude and $(B-V)$ color from Montgomery et al. (1993), where available⁸, number of RV measurements in the WIYN (N_W) and CfA (N_C) samples (counting RVs for primary stars only), the modified Julian date (JD - 2400000) of the first observation (JD_0) and last observation (JD_f), the weighted mean RV (\overline{RV} ; for binaries with orbital solutions, we instead provide the center-of-mass, γ -RV) and the weighted standard error of the mean RV (RV_e ; for binaries with orbital solutions we instead provide the error on the γ -RV), the combined RV precision (i , defined as in Hole et al. 2009) the RV membership probability (P_{RV} , defined in Section 5.2), the proper-motion membership probabilities from Yadav et al. (2008, P_{PM_y}), Zhao et al. (1993, P_{PM_z}), Girard et al. (1989, P_{PM_g}) and Sanders (1977, P_{PM_s}), where available, the e/i and $P(\chi^2)$ values (defined in Section 5.1), the membership classification (see Section 5.3) and finally a comment field.

We mark particularly notable stars within our stel-

⁶ We follow the same method as Hole et al. (2009) to define WOCS ID based on the given star’s V magnitude and distance from the cluster center.

⁷ If available the cross-reference ID is taken from Sanders (1977) and denoted by the prefix “S”. If there is no Sanders (1977) source match, we provide the Montgomery et al. (1993) ID, if available, denoted by the prefix “M”. If both of those studies lack a source match, we provide the Fan et al. (1996) IDs, if available, denoted by the prefix “F”. There are 13 sources in our table that do not have matches in these three references. As with all sources, we provide their RA and Dec positions for matching to other catalogs.

⁸ For the few stars in our sample that are not in the Montgomery et al. (1993) survey and for which we can find no other BV photometry from the literature, we derive V magnitudes from the 2MASS JHK photometry using a similar relationship to Girard et al. (2004). For these stars, we do not have $(B-V)$ colors. The stars with IDs that have a prefix of “T” are taken from Mathieu et al. (1986) who use photometry from Murray & Clements (1968).

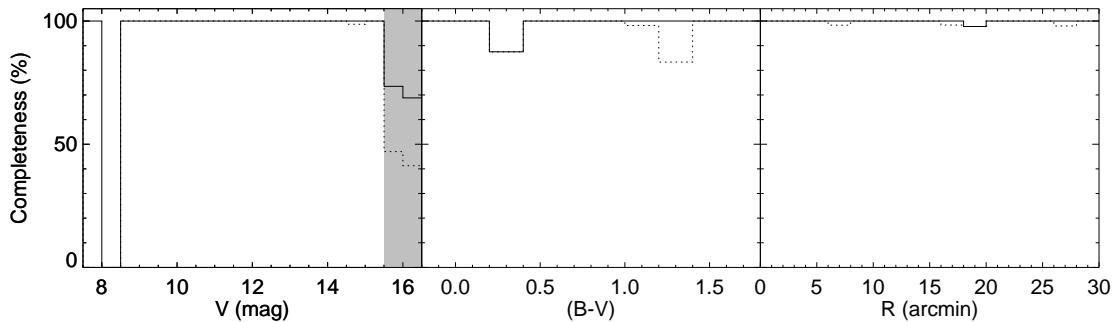


FIG. 6.— Completeness histograms as a function of apparent V magnitude (left), $(B-V)$ color (middle) and radius from the cluster center (right) for stars observed in M67. In the V completeness panel we show all stars observed in this survey. The gray region shows stars that are fainter than our primary sample selection of $V \leq 15.5$. (Note that there are only two stars brighter than $V = 8.5$ in our sample, both of which are proper-motion non-members and neither of which have ≥ 3 observations, as discussed in the main text.) In the $(B-V)$ and radius panels we show our completeness for stars in this primary sample only. In all plots the percentage of stars observed ≥ 1 time is plotted with the solid line, while the percentage of stars observed ≥ 3 times is plotted with the dotted line.

lar sample in this comment field of Table 4. X-ray sources identified by Belloni et al. (1998) with ROSAT are labeled with “X” followed by the source number given in their paper. Likewise X-ray sources identified by VandenBerg & Stetson (2004) with Chandra are labeled with “CX” followed by the source number given in their paper. Photometric variables (Gilliland et al. 1991; Stassun et al. 2002; van den Berg et al. 2002; Sandquist & Shetrone 2003a,b; Sandquist et al. 2003; Qian et al. 2006; Bruntt et al. 2007; Stello et al. 2007; Pribulla et al. 2008; Yakut et al. 2009) are labeled with “PV”, or “PV?” if the authors identify the photometric variability as uncertain (e.g., possible flare event detections, possible nearby source contamination, etc.). We also label the W UMA’s found in M67, and provide the GCVS names for photometric variables, where available (e.g., AH Cnc, ES Cnc, etc.). Stars that are rotating significantly more rapidly than our instrumental resolution of $\sim 10 \text{ km s}^{-1}$ are labeled as “RR”. Sources that are detected as triple systems are labeled with “triple”. Additionally, we label blue stragglers with “BSS”, “yellow giants” with “YG”, and the two sub-subgiants with “SSG”. We briefly discuss a few of these notable stellar populations in Section 6.2.

5.1. Radial-Velocity Variability

We identify binaries in our M67 data using the e/i statistic, which is the ratio of the standard deviations (e) to the expected precision (i) of the RVs for a given star. Members of binaries with orbital periods short enough to show significant RV variation in our data will have higher standard deviations than expected for single stars. Therefore high e/i values indicate binaries or higher-order systems. As a large number of stars in our sample have RV measurements from multiple telescopes, and therefore multiple precision values, we use the formalism from Bevington & Robinson (1992) to derive the e and i values for data with multiple precision values, as in Hole et al. (2009).

We derive an e/i value for all single-lined stars with ≥ 3 RV measurements. Previous work by Geller et al. (2008) shows that stars with $e/i > 4$ can be securely identified as binaries (or higher-order systems), and we initially fol-

lowed this same cutoff for identifying binaries here. In practice, however, we have derived RV orbital solutions for all proper-motion members in our primary sample with $3 \leq e/i < 4$. (There are only three proper-motion non-members in our primary sample with $3 \leq e/i < 4$; each of these have mean RVs outside of the cluster distribution.) Therefore here, we identify binaries in our data as having $e/i \geq 3$.

The uncertainties for RVs in double-lined (SB2) binaries are not well established, and therefore we do not derive e/i values for these stars. Instead we identify SB2s as binaries directly by inspection of the spectra and the morphology of the peaks of the cross-correlation functions. (We derive the uncertainties on the mean RVs, RV_e , for SB2s without orbital solutions using the measurement precisions that we derive above for single-lined stars; we suspect that the RV uncertainties for such SB2s quoted here are in fact lower limits.)

In addition to the e/i statistic, we also provide the $P(\chi^2)$ value. This statistic tests the hypothesis that a given star’s distribution of RVs is consistent with a constant value at the mean RV. Members of binaries with short enough orbital periods to show significant RV variations in our data will be inconsistent with a constant RV and therefore will have small $P(\chi^2)$ values. To derive the $P(\chi^2)$ value, we first calculate the standard χ^2 statistic, using the weighted mean RV and the respective precision of each RV measurement (discussed in Section 3.1). For each observed star, we use the number of RV measurements minus one for the degrees of freedom. Then $P(\chi^2)$ is the corresponding probability for obtaining a value of χ^2 greater than or equal to the observed value with the given degrees of freedom. Again, we only derive $P(\chi^2)$ values for single-lined stars with ≥ 3 measurements.

In the following analysis we will identify binaries by having $e/i \geq 3$, or having a binary orbital solution. (The additional $P(\chi^2)$ statistic is provided for interested readers who prefer to use these values to perform their own selection of binaries.) All stars with $e/i < 3$ for which we have not derived binary orbital solutions, are labeled as “single”. However, some of these stars are undoubtedly in long-period binaries, currently beyond our detection limit.

TABLE 2
GAUSSIAN FIT PARAMETERS FOR CLUSTER AND FIELD
RADIAL-VELOCITY DISTRIBUTIONS

Parameter	Cluster	Field
Ampl. (Number)	147.8 ± 0.7	2.38 ± 0.10
RV (km s ⁻¹)	33.615 ± 0.005	23.4 ± 2.2
σ (km s ⁻¹)	0.854 ± 0.005	46.7 ± 2.2

Finally, we also identify five likely triple stars in our sample, and label them as such in Table 4. In most cases the systems are double lined, where the RVs for one star vary on a much shorter time scale than those of the other star. For a few, we see hints of tertiary velocities at low signal-to-noise, but we have yet to analyze these spectra in detail to derive all three velocities simultaneously. Additional triple stars may be detectable in our sample, for instance within the RV residuals from binary orbital solutions, but we save this analysis for a future paper.

5.2. Membership

In Figure 7 we show the distribution of weighted mean RVs for all stars in our sample with ≥ 3 RV measurements and $e/i < 3$, and γ -RVs for binaries with orbital solutions. For stars with RVs from multiple telescopes, we use the respective RV precision values to calculate the weighted means, and use those results here. The cluster RV distribution is clearly distinguished from that of the field as the narrow distribution peaked at a mean RV of +33.6 km s⁻¹.

In order to derive membership probabilities, we first fit simultaneous one-dimensional Gaussian functions to the cluster and field RV distributions, $F_c(v)$ and $F_f(v)$, respectively. (We exclude from this fit binaries without orbital solutions, as their γ -RVs are unknown.) The resulting combined fit to the cluster and field distributions are shown in the blue line in the left panel of Figure 7, and the fit parameters are given in Table 2 (fit to a histogram with a bin size of 0.5 km s⁻¹). We then use the following equation,

$$P_{\text{RV}}(v) = \frac{F_c(v)}{F_f(v) + F_c(v)} \quad (1)$$

(Vasilevskis et al. 1958) to calculate the RV membership probability $P_{\text{RV}}(v)$ for a given star in our sample.

We only compute membership probabilities for stars with ≥ 3 observations. For non-RV-variable stars, we use the weighted mean RV in the calculations. For binaries with orbital solutions, we use the γ -RV. For RV-variable stars without orbital solutions, we cannot calculate a reliable RV membership probability, as the γ -RV is unknown. For these stars we instead provide a preliminary membership classification, described in Section 5.3.

We plot the resulting distribution of RV membership probabilities in the right panel of Figure 7. Cluster and field stars are cleanly separated, and we choose a cutoff of $P_{\text{RV}} \geq 50\%$ to define our M67 cluster member sample. Using our sample of single cluster members with $e/i < 3$ and binary cluster members with orbital solutions, we find a mean cluster velocity of +33.64 km s⁻¹ (with an internal precision of ± 0.03 km s⁻¹), in good agreement with previous RV surveys (e.g., see Yadav et al. 2008, and references therein).

As stated in Sections 3 and 4, the RVs in this paper are all on the native CfA system, which is found to be shifted by -0.14 km s⁻¹ compared to the IAU system. Therefore, the mean cluster velocity quoted here may also have this offset compared to the IAU system (i.e., +0.14 km s⁻¹ may need to be added to our velocities to get onto the IAU system).

The ratio of the areas under the Gaussian fits to the cluster and field distributions provides an estimate of the field star contamination. At a membership probability of 50%, we expect a 3.5% contamination from field stars in our RV cluster member sample (i.e., ~ 20 stars).

5.2.1. Comparison of Radial-Velocity and Proper-Motion Membership Probabilities

Here we compare with four published proper-motion membership catalogs for M67: Sanders (1977), Girard et al. (1989), Zhao et al. (1993) and Yadav et al. (2008). For this comparison we use only non-RV variable stars and binaries with orbital solutions in our primary sample (thereby excluding binaries whose γ -RVs are unknown) so as to ensure secure RV membership probabilities. There are 836 stars in our primary sample that meet these criteria.

We find excellent agreement with all four proper-motion sources. There are 456 stars in this sample with Sanders (1977) proper-motion membership probabilities $\geq 50\%$, of which 430 (94%) also have RV membership probabilities $\geq 50\%$. 410 stars in this sample have Girard et al. (1989) proper-motion membership probabilities $\geq 50\%$, of which 396 (97%) also have RV membership probabilities $\geq 50\%$. 164 stars in this sample have Zhao et al. (1993) proper-motion membership probabilities $\geq 50\%$, of which 149 (91%) also have RV membership probabilities $\geq 50\%$. Finally, 330 stars in this sample have Yadav et al. (2008) proper-motion membership probabilities $\geq 50\%$, of which 200 (91%) also have RV membership probabilities $\geq 50\%$. If we examine stars in this sample that have proper-motion membership probabilities of $\geq 50\%$ from all four references, we find that 95/100 (95%) also have RV memberships $\geq 50\%$.

For stars with both RV and proper-motion membership probabilities, we combine the results to further refine our cluster member sample. We first take all stars that have RV membership probabilities $\geq 50\%$ as candidate cluster members. We then examine the available proper-motion membership probabilities for each star to remove non-members from this sample. For each proper-motion reference we assign the same cutoff of $\geq 50\%$ membership probability to denote cluster members. If the available proper-motion membership values for a given star all indicate that the star is a non-member, we remove it from our cluster member sample. For stars with proper-motion membership probabilities from multiple references that disagree on membership status, we allow each proper-motion reference one “vote” on membership (either member or non-member) and take the majority vote to determine the proper-motion membership status. If this procedure results in a tie, we instead use the result from the highest precision proper-motion membership survey for the given star to determine membership (in the order of Girard et al. 1989, Yadav et al. 2008, Zhao et al. 1993, then Sanders 1977, with Girard et al. 1989 at the highest precision).

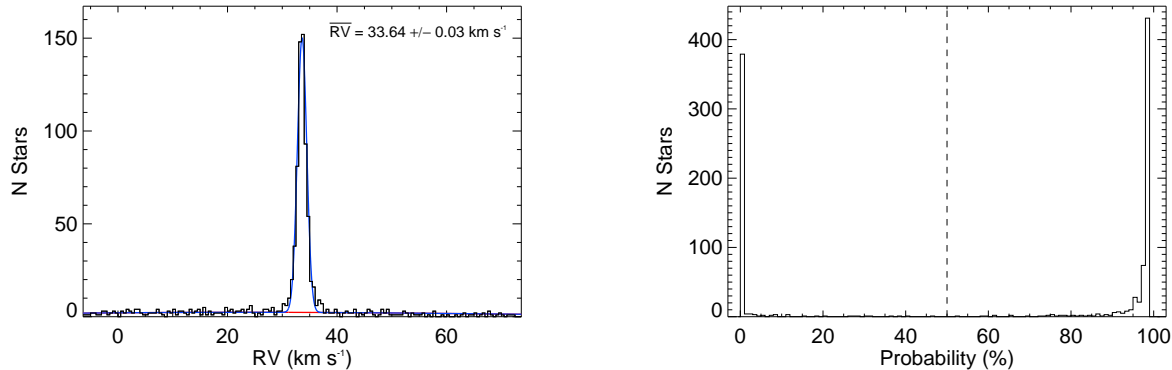


FIG. 7.— RV distribution (left) and the distribution of RV memberships (right) for stars in our M67 stellar sample. To derive the RV distribution we use the weighted mean RVs for stars with ≥ 3 observations with $e/i < 3$, and γ -RVs for binaries with orbital solutions. (Here we exclude detected binaries without orbital solutions, because their γ -RVs are unknown.) We use bins of 0.5 km s^{-1} . The red line shows the field component to our simultaneous two-Gaussian fit to the observations, and the blue line shows the combined fit of the cluster and field distributions, which we use to derive the membership probabilities for observed stars in M67. On the right, we show a histogram of RV memberships (rounded to the nearest percent) of the same stars used in constructing the RV distribution. RV members are defined as having $P_{RV} > 50\%$.

In practice, only 24 stars in our primary sample have proper-motion membership probabilities that result in a “tie”, all but two of which have only two proper-motion membership values. Also for reference, there are 35 stars in our primary sample with proper-motion memberships from all four studies where one disagrees with the other three. In 23 of these cases, Zhao et al. (1993) is the outlier. In 8 of these cases, Yadav et al. (2008) is the outlier. In 4 of these cases, Girard et al. (1989) is the outlier.

Of the 515 stars in our primary sample that have secure RV memberships $\geq 50\%$ (i.e., SM and BM stars, see Section 5.3) and proper-motion measurements, 455 pass this proper-motion membership test, and are therefore deemed bona fide cluster members. This $\sim 12\%$ contamination of our RV member sample is about 3.5 times larger than we estimate above based solely on the RV distributions of the cluster and field stars. We note that 75% of these RV members that we determine to be proper-motion non-members from the algorithm above reside outside of 15 arcmin from the cluster center. Also about 23% of these RV members that are proper-motion non-members have at least one proper-motion membership value (from one of the references above) greater than 50%. However, to minimize possible field star contamination, we remove all of these proper-motion non-members from our cluster member sample.

5.3. Membership Classification of Radial-Velocity Variable Stars

For stars that show no significant RV variability and binaries with orbital solutions, we can calculate precise RV membership probabilities that allow us to separate cluster members from field stars, as described above. However, for binary stars that do not have RV orbital solutions, we cannot calculate reliable RV membership probabilities because we do not know their γ -RVs. Thus we follow a similar method to Geller et al. (2008, 2010) and Hole et al. (2009) in order to provide a qualitative classification of the membership and variability for each observed star.

Our classification scheme is defined in Table 3, where we identify our eight qualitative membership classes, the

selection criteria for each class, and also the number of stars that reside in each class. The selection criteria depend on the number of RVs, the e/i value, the RV membership probability (P_{RV} , determined either using the mean RV, \overline{RV} , or the γ -RV, for binaries with orbital solutions), and the proper-motion membership “vote” described in Section 5.2.1. For the proper-motion membership vote, we use “ $P_{PM}=M$ ” to indicate proper-motion members, and “ $P_{PM}=NM$ ” to indicate proper-motion non-members. If a star does not have a proper-motion measurement, we use only the RV criteria to classify the star.

In short the single members/non-members (SM/SN) or binary members/non-members (BM/BN) are stars with secure membership status; these are the only stars for which we can provide reliable RV membership probabilities. For RV variable stars with ≥ 3 RV measurements that do not have a binary orbital solution, we divide our classification into three groups, including binary likely members (BLM), binaries with unknown RV membership (BU) and binary likely non-members (BLN). We anticipate that eventually orbital solutions derived for BLM binaries will place them in the BM category, while those for the BLN binaries will place them in the BN category (since many of these sources are proper-motion non-members, and for those that are not, it is unlikely that an orbital solutions will place their γ -RVs within the cluster distribution). Binaries with unknown RV membership (BU’s) are proper-motion members. Therefore here we assume that these are indeed cluster members (unlike in other WOCS papers, where proper-motion memberships were unavailable). Stars with < 3 RV measurements have unknown RV membership (U), as these stars do not meet our minimum criterion for deriving RV memberships or e/i values. In the following analyses we restrict our cluster member sample to only include the 562 stars classified as either SM, BM, BLM or BU.

Finally, as mentioned above, stars that show broadened spectral features (e.g., due to rapid rotation) do not have secure single-measurement RV precision values, and therefore in most cases we cannot confidently classify such stars as binaries or singles. We provide our best

TABLE 3
DESCRIPTION OF STARS OR STAR SYSTEMS WITHIN EACH MEMBERSHIP CLASS

Class	Description	Criteria	Number
SM	Single Member	≥ 3 RVs, $e/i < 3$, $P_{RV}(\overline{RV}) \geq 50\%$ AND $P_{PM} = M$	420
SN	Single Non-member	≥ 3 RVs, $e/i < 3$, $P_{RV}(\overline{RV}) < 50\%$ OR $P_{PM} = NM$	498
BM	Binary Member	binary orbit, $P_{RV}(\gamma\text{-RV}) \geq 50\%$ AND $P_{PM} = M$	108
BN	Binary Non-member	binary orbit, $P_{RV}(\gamma\text{-RV}) < 50\%$ OR $P_{PM} = NM$	17
BLM	Binary Likely Member	≥ 3 RVs, $e/i \geq 3$, $P_{RV}(\overline{RV}) \geq 50\%$ AND $P_{PM} = M$	23
BU	Binary with Unknown RV Membership	≥ 3 RVs, $e/i \geq 3$, $P_{RV}(\overline{RV}) < 50\%$ AND the range in RV measurements includes the cluster mean RV AND $P_{PM} = M$	11
BLN	Binary Likely Non-Member	≥ 3 RVs, $e/i \geq 3$, $P_{RV}(\overline{RV}) < 50\%$ AND all RV measurements are either at higher or lower RV than the cluster distribution, OR $P_{PM} = NM$	58
U	Unknown RV Membership	< 3 RVs	143

assessment of the binarity of these sources in Table 4 and indicate our uncertainty in their class with parentheses, e.g. (BL)M, (S)N, etc.

6. DISCUSSION

In the following section, we use our confirmed cluster members to investigate the CMD (Section 6.1), identify and discuss a few notable stellar populations (Section 6.2), analyze the spatial distribution of the single, binary, giant and BSS cluster populations (Section 6.3) and derive the velocity dispersion of the solar-type stars in our cluster member sample (Section 6.4).

6.1. Color-Magnitude Diagram

In Figure 8 we plot the CMD of all stars in our stellar sample with $V < 15.5$ (and available $(B-V)$ colors; left) and only the confirmed cluster members within the same magnitude range (right). Without removing non-members, the main-sequence of the cluster is visible, but the BSS and giant populations cannot be distinguished from the field. Applying both our proper-motion and RV membership criteria reveals a rich cluster containing well populated main-sequence, subgiant and giant branches as well as a large population of BSS (blue points), four yellow giants (red points), and two sub-subgiants (green points). Specifically, we plot here stars that we classify as SM, BM, BLM and BU, and we also include here stars in the U category as well as rapid rotators that are proper-motion members.

For comparison, we also plot a 4 Gyr isochrone and a zero-age main-sequence isochrone (solid lines), as well as an equal-mass binary line (dashed line). The isochrones are from Marigo et al. (2008), and use solar metallicity, $(m - M)_V = 9.6$ and $E(B - V) = 0.01$, consistent with recent results derived in the literature (see Section 1). We include the isochrones simply to help guide the eye; they are not meant as a fit to the observed data.

Binaries with orbital solutions are circled, and binaries without orbital solutions are marked with diamonds. As is seen clearly here, and also noted by Latham & Milone (1996) and Latham (2007), the “exotic” stars (i.e., the BSS, yellow giants, and sub-subgiants) have a remarkably high binary frequency. In total we identify 14 BSS, four yellow giants (one of which is outside of a 30 arcmin radius from the cluster center) and two sub-subgiants in our stellar sample. At least 16/20 (80% \pm 20%) of these exotic stars are RV variables (and others may also be binaries, e.g. with long-period orbits that are currently

outside of our detection limit). In comparison, 122/538 (22.7% \pm 2.1%) of the “normal” stars, located in more typical positions in the CMD, show RV variability indicative of binarity. Thus the exotic stars have a significantly higher frequency of binaries than the normal stars. This result is similar to that found in the old (7 Gyr) open cluster NGC 188, where Mathieu & Geller (2009, 2015) find that 80% of the NGC 188 BSS have binary companions (roughly three times the binary frequency of the main-sequence stars in NGC 188).

We also note the very tight red giant sequence, first discussed in detail by Janes & Smith (1984). Such a tight red giant sequence is expected for a single coeval population, but, interestingly, the giants of NGC 188 (e.g. Geller et al. 2008) and the intermediate-age (2.5 Gyr) open cluster NGC 6819 (e.g. Hole et al. 2009) show a much larger scatter than the giants in M67. The origin of the scatter in these other open clusters is unknown.

6.2. Stars of Note

Within our cluster member sample, there are a number of intriguing stellar populations, from those that lie far from the predicted locus of single stars from stellar evolution theory (including the well known BSS, Section 6.2.1, and anomalous giants, Section 6.2.2), to those that have physical characteristics very similar to those of our Sun (Section 6.2.3), and even three exoplanet host stars (Section 6.2.4). In the following we briefly identify and discuss these stars of note.

6.2.1. Blue Stragglers

M67 is home to one of the most well-studied BSS populations (see, e.g., Eggen 1981; Peterson et al. 1984; Mathieu et al. 1986; Manteiga et al. 1989, 1991; Gilliland & Brown 1992; Leonard & Linnell 1992; Milone 1992; Milone & Latham 1994; Leonard 1996; Landsman et al. 1997, 1998; Deng et al. 1999; Shetrone & Sandquist 2000; Hurley et al. 2001; van den Berg et al. 2001; Sandquist et al. 2003; Chen & Han 2004; Hurley et al. 2005; Sandquist 2005; Zhang et al. 2005; Andronov et al. 2006; Tian et al. 2006; Bruntt et al. 2007; Latham 2007; Liu et al. 2008; Pribulla et al. 2008; Lu et al. 2010). In total, we identify 25 candidate BSS that are discussed in the literature: 1006 (S1066), 1007 (S1284), 1010 (S977), 1017 (S1466), 1020 (S751), 1025 (S1195), 1026 (S1434), 2007 (S984), 2008 (S1072), 2009 (S1082), 2011 (S968), 2013 (S1267), 2015 (S792), 2068 (S277), 3005 (S1263), 3009 (S1273),

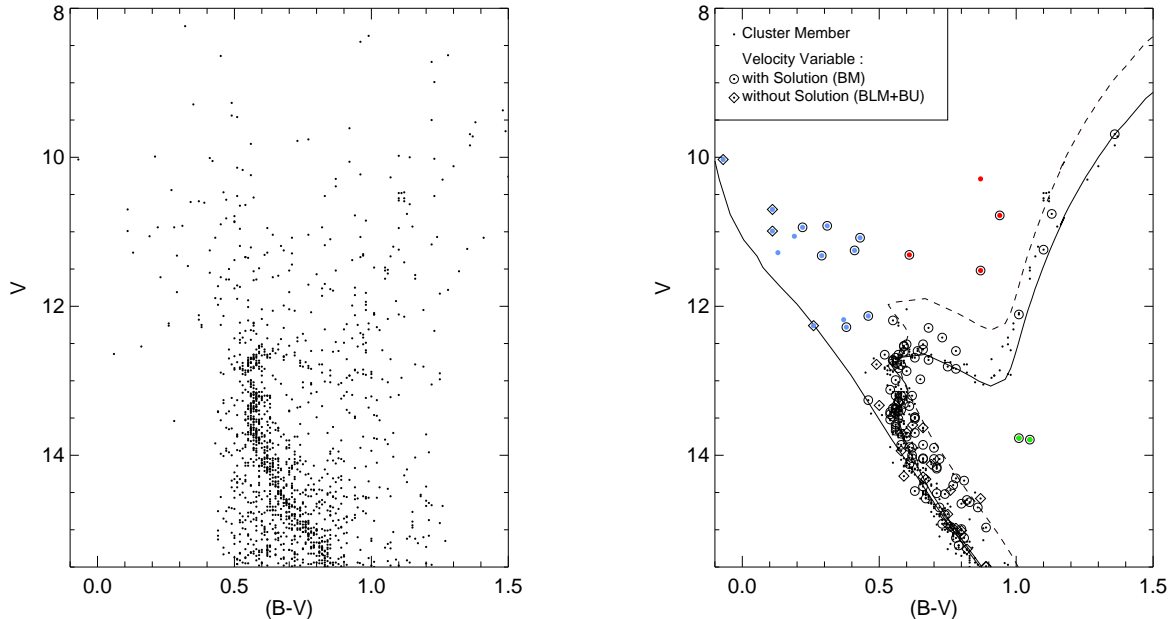


FIG. 8.— Color-magnitude diagrams for all stars in our M67 stellar sample with $V < 15.5$ (and available $(B-V)$ colors; left) and only cluster members within the same magnitude range (right). We take here as cluster members all stars that reside in the SM, BM, BLM, and BU classes, as well as stars in the U class and rapid rotators that are proper-motion members (see Section 5.3). Binary members with orbital solutions (BMs) are circled, and velocity variables without orbital solutions that are likely cluster members (BLMs and BUs) are shown in diamonds. For comparison, in the right panel we also plot a zero-age main-sequence isochrone and a 4 Gyr isochrone (solid lines Marigo et al. 2008) using $(m-M)_V = 9.6$, $E(B-V) = 0.01$ and solar metallicity. We also plot the equal-mass binary locus (dashed line) obtained by shifting the 4 Gyr isochrone by -0.75 mag.

3010 (S975), 3013 (S752), 4003 (S1036), 4006 (S1280), 5005 (S997), 5071 (S145), 6038 (S2226), 8006 (S2204), 9005 (S1005).

We find 1017 and 5071 to be cluster non-members based on kinematic membership information, and therefore we remove these from the list of BSS. 1017 is a non-member by both proper motions and RVs. 5071 has a proper-motion membership probability of 94% from Sanders (1977), but the star appears to be single with a mean RV of 39.79 ± 0.12 km s $^{-1}$, which results in a 0% RV membership probability.

By examination of the CMD shown in Figure 8, we remove an additional nine stars from the BSS sample. 1020, 4003, 8006 and 9005 lie close to the blue hook of the cluster (given the Montgomery et al. 1993 BV photometry), and therefore we conservatively exclude these stars from our BSS sample. 2007, 2015, 2068 and 3009 are above the turnoff, but reside in a region expected to be populated by binaries containing normal main-sequence turnoff stars. We only detect a binary companion to 2068. However, the remaining three stars may have long-period companions, currently beyond our detection limit, with high enough masses to explain their location on the CMD. We therefore do not include these stars in our BSS sample. 2008 is the reddest BSS candidate in this sample, residing ~ 1.5 magnitudes directly brighter than the main-sequence turnoff. The BSS status of 2008 is somewhat ambiguous, as it may currently be evolving toward the giant branch. We choose to exclude 2008 from our BSS sample and will include it in our “anomalous giant” sample discussed below. (Mathieu & Latham 1986 also exclude 2008 from their BSS sample based on similar arguments.)

Thus in total we find M67 to have 14 BSS in our primary stellar sample. Remarkably, 11 of these 14 BSS show significant RV variations indicative of binary companions. Seven of these BSS have secure orbital solutions, and an additional two rapidly rotating BSS (1026, 4006) have preliminary orbital solutions. The detected binary frequency amongst the M67 BSS is $79\% \pm 24\%$. This high binary frequency for the M67 BSS is similar to that found in the old (7 Gyr) open cluster NGC 188 (Mathieu & Geller 2009), and in the field (Carney et al. 2001). We will discuss these BSS in detail, including their binary properties, in a subsequent paper.

6.2.2. Anomalous Giant Stars

There are six stars with $(B-V)$ colors consistent with the subgiant or giant branches but have magnitudes and/or chemical abundances that set them apart from the more typical giants along the isochrone shown in Figure 8. We discuss these anomalous giant stars below.

Sub-subgiants: 15028 (S1113) and 13008 (S1063) are fainter than the subgiant branch but redder than the main-sequence. These sub-subgiants are both members of binary systems and are also X-ray sources. Their origins are unknown, and we refer the reader to Mathieu et al. (2003) for a very detailed discussion on the available observations for these stars.

Lithium-rich Subgiant: Canto Martins et al. (2006) find the subgiant 6008 (S1242) to have an anomalously high Lithium abundance as compared to normal main-sequence turnoff stars in the cluster, although it falls within the normal subgiant branch on the CMD. We confirm the membership of 6008, and we also confirm that 6008 is in a binary.

Yellow Giants: 1015 (S1237), 1112, 2002 (S1040) and 2008 (S1072) are all brighter than the giant branch and have often been referred to as “yellow giants”. 1112 is 55.6 arcmin from the cluster center, and is therefore not included in our primary stellar sample. This star shows no evidence for a binary companion. The other three yellow giants are all members of binaries. 2002 was studied in detail by Landsman et al. (1997, 1998) who find the secondary to be a low-mass He white dwarf, suggesting that the system went through an episode of mass transfer while the donor was on the giant branch. Therefore 2002 may have been a BSS in the recent past, and is now in the process of evolving towards the giant branch. 2008 may also have previously been a BSS that is now evolving towards the giant branch (Mathieu & Latham 1986). A similar evolutionary scenario may explain the anomalous CMD location of 1015.

6.2.3. Solar Twins

M67 is of a similar age and chemical composition to the Sun, and is therefore an ideal target for investigating solar analogs (Pasquini et al. 2008; Reiners & Giampapa 2009; Giampapa et al. 2006; Castro et al. 2011; Önehag et al. 2011). Stars 7003 (S1041), 10018 (S1462), 11018 (S1095), 12012 (S996), 13021 (S945), 14014 (S779), 16011 (S770), 16023 (S2211), 17026 (S1335), and 18013 (S785) were found to have effective temperatures consistent with the Sun, and are the closest analogs to the Sun in M67. We confirm that these 10 stars are cluster members, and all but one appear to be single (with 10018 at $e/i=4.19$). 16023 was found to be a photometric variable by Stassun et al. (2002), although variability was only detected above the 3σ level in the B band (and not in V or I). We find 16023 to have $e/i=0.93$.

6.2.4. Exoplanet Host Stars

Brucalassi et al. (2014) identify three stars hosting roughly Jupiter-mass exoplanets in M67: 1045 (S364), 13014 (S802) and 16011 (S770). Our measurements are not sensitive enough to detect such low-mass companions, but we confirm that none appear to have stellar-mass companions and that all three are cluster members. We also note that 1045 is an X-ray source (X19 from Belloni et al. 1998).

6.3. Radial Distribution of Cluster Members

The spatial distribution of stars in M67 has been studied in detail (e.g. Mathieu & Latham 1986; Zhao et al. 1996; Sarajedini et al. 1999; Bonatto & Bica 2003; Davenport & Sandquist 2010). M67 is mass segregated, as is expected for a 4 Gyr cluster with a half-mass relaxation time of 100 Myr (Mathieu & Latham 1986). In light of our new RV memberships and identification of binaries, we briefly re-investigate the spatial distribution of cluster member populations using our primary sample. In Figure 9 we show the projected radial distribution for the single main-sequence stars, binary main-sequence stars, single giants and BSS. Singles are stars classified as SM, and binaries are classified as either BM, BLM or BU.

A Kolmogorov-Smirnov (K-S) test shows that the main-sequence binaries are centrally concentrated with

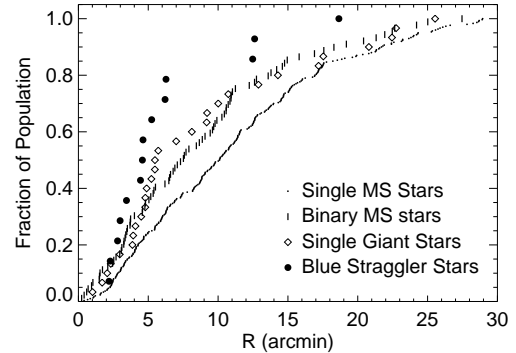


FIG. 9.— Cumulative projected radial distribution of cluster members in M67. We divide our primary sample into single and binary main-sequence (MS) stars, single giants and blue stragglers. The giants are identified as having $(B - V) > 0.9$, and we exclude the anomalous giants discussed in Section 6.2. The blue straggler sample is identified as discussed in Section 6.2 and shown in Figure 8. Both the binaries and blue stragglers are significantly centrally concentrated with respect to the single main-sequence stars.

respect to the main-sequence single stars at the 98.7% confidence level. Comparing all single stars to all binaries shows that the binaries are more centrally concentrated at the 99.8% confidence level. Because the total mass of a given binary is generally more massive than that of a single star in our primary sample, this result confirms that M67 is mass segregated.

Mathieu & Latham (1986) find the BSS to be centrally concentrated with respect to the single stars near the cluster turnoff. Our BSS sample is slightly different than that of Mathieu & Latham (1986). Nonetheless, the result is the same. A K-S test comparing the BSS to the single main-sequence stars show that the BSS are centrally concentrated at the 99.7% confidence level. This result suggests that the BSS are more massive than the main-sequence stars in the cluster, as was noted by Mathieu & Latham (1986).

In many globular clusters and also the old open cluster NGC 188, BSS show a bimodal projected radial distribution (e.g. Ferraro et al. 1997, 2012; Mapelli et al. 2006; Geller et al. 2008). We do not observe evidence for a bimodal radial distribution in our M67 BSS sample. However, our sample only extends to 6 or 7 core radii. In NGC 188, which is of a similar dynamical age to M67, the halo BSS population begins at roughly 6 core radii and extends to about 13 core radii (at least). Thus if M67 and NGC 188 have similar BSS radial distributions, we would only expect to see the inner population of M67 in our current sample, and would require a survey extending to roughly twice the current radial extent to search for a bimodal structure.

Interestingly, the giants appear to follow a similar spatial distribution as the binaries, despite having very similar masses to the upper main-sequence stars included in our primary sample. However, given the relatively small sample size of the single giants, a K-S test comparing the spatial distributions of the single giants and single main-sequence stars returns a distinction at only the 95.9% confidence level. For comparison, the NGC 188 giants do not follow the distribution of the binaries, and instead follow closely to the single cluster members (see Figure 9

in Geller et al. 2008), both when considering the entire spatial extent of the RV survey and when limiting to a similar number or core radii as our M67 sample. This difference is intriguing, but the small sample sizes of the giants in both clusters make such comparisons uncertain.

6.4. Cluster Radial-Velocity Dispersion and Virial Mass

We follow the method of Geller et al. (2010) to calculate the RV dispersion of the M67 single main-sequence, subgiant and giant members in our primary sample. (We exclude the binaries and BSS because these have significantly different spatial distributions, likely due to their higher masses.) This method assumes that the observed RV dispersion is composed of two components, one which we will call the “combined RV dispersion” and one for the observational error, and also assumes that the distributions of RVs and errors are Gaussian. The observed dispersion is directly measured, and by subtracting off the component from observational error, we recover the combined RV dispersion. The combined RV dispersion itself contains contributions from both the true RV dispersion of the cluster and undetected binaries, which also artificially inflates the observed RV dispersion. We aim to recover the true RV dispersion from our data.

First we calculate the observed RV dispersion, which is simply the standard deviation of the observed mean RVs for each star about the cluster mean RV (calculated in Section 5.2). In our calculation, we use the weighted mean RVs for each star in the given sample (see Table 4), which utilize the single-measurement precision values from the given telescope for each individual RV value (see Section 3.1). For the single main-sequence, subgiant and giant stars in our primary sample, the resulting observed velocity dispersion is $0.86 \pm 0.11 \text{ km s}^{-1}$. After correcting for the observational error (following the method of McNamara & Sanders 1977 and McNamara & Sekiguchi 1986), we find a combined RV dispersion of $0.80 \pm 0.04 \text{ km s}^{-1}$.

We then follow a similar method to that of Geller et al. (2010) to correct this combined RV dispersion for the contribution from undetected binaries. Briefly, we run a Monte Carlo analysis to create many realizations of our M67 observations. For each realization, we generate a population of synthetic single and binary stars (given an input binary frequency), and produce synthetic RVs for these stars on the true observing dates from our M67 survey, which we analyze in the same manner as our real observations. We run this analysis for a range of true RV dispersion values, and for each value, we derive the difference between the synthetic combined RV dispersion and the input true RV dispersion. This difference is the contribution from undetected binaries (β in Equation 5 of Geller et al. 2010).

For this analysis, we improve upon the technique of Geller et al. (2010) in our treatment of the binaries, and therefore, for clarity, we explain the method in some further detail here. In order to recover the true velocity dispersion, we must also estimate the binary frequency of the cluster. We use a similar Monte Carlo method to Geller & Mathieu (2012) to account for our incompleteness in binary detections out to the hard-soft boundary. As in Geller & Mathieu (2012), we assume that the orbital parameters of the M67 binaries follow the same distributions as observed for the solar-

type binaries in the Galactic field from Raghavan et al. (2010), except here we use a circularization period of 12.1 days (Meibom & Mathieu 2005). We also make a few updates to the method of Geller & Mathieu (2012). First, rather than choosing one specific primary mass, we draw from an inferred primary-mass distribution within our M67 primary sample (derived by comparisons to a Marigo et al. 2008 isochrone). Second, we attempt to recreate the correlation between binary mass ratio and orbital period observed for field binaries by Raghavan et al. (2010, see Figure 17 and related discussion). Specifically, for binaries with periods between 100 days and 1000 years, we choose mass ratios from a uniform distribution with 10% of systems having a mass ratio of unity (e.g., twins). For binaries with periods greater than 1000 years we draw mass ratios from a uniform distribution limited to be less than 0.95. For binaries with periods less than 100 days, we enforce $\sim 19\%$ to have mass ratios between 0.2 and 0.45, $\sim 44\%$ to have mass ratios between 0.45 and 0.9, and the remainder to have mass ratios between 0.9 and 1, all drawn from uniform distributions between the respective mass ratio limits. Finally, we limit the field log-normal orbital period distribution so that the binaries are detached (using radii estimates from a Marigo et al. 2008 isochrone), and the periods are less than the hard-soft boundary.

The assumed location of the hard-soft boundary, which is at roughly 10^5 - 10^6 days in M67, is especially important for the undetected binary correction. We do not expect to detect binaries at these long periods. Furthermore, the hard-soft boundary is near the peak of the log-normal distribution, and therefore the assumed binary frequency is particularly sensitive to this cutoff. We estimate the hard-soft boundary as the location where a synthetic binary’s binding energy is equal to the kinetic energy of a “typical” star moving at an assumed velocity dispersion. For the mass of this typical star, we take the mean mass of an object (single or total mass of a binary) from the Hurley et al. (2005) N -body simulation of M67, which at 4 Gyr is $0.95 M_{\odot}$. We then assume a velocity dispersion, run our analysis to derive the true velocity dispersion in our M67 sample (given the resulting hard-soft boundary and total binary frequency), and iterate until this assumed velocity dispersion is $< 0.05 \text{ km s}^{-1}$ different from the derived true velocity dispersion in M67 (a somewhat arbitrary limit meant to be roughly equivalent to the precision with which we can measure the velocity dispersion). As a starting guess, we use the combined dispersion value of 0.80 km s^{-1} , found above.

Our analysis of the single main-sequence, giant and sub-subgiant stars in this sample requires only two iterations. The resulting orbital period distribution matches closely to those predicted by the N -body open cluster models of Hurley et al. (2005) and Geller et al. (2013), and we estimate the total binary frequency in our sample to be $57\% \pm 4\%$. We derive a true velocity dispersion, after correcting for measurement error and undetected binaries, for the M67 single main-sequence stars, subgiants and giants with $V \leq 15.5$ of $0.59^{+0.07}_{-0.06} \text{ km s}^{-1}$.

Using a subsample of 20 of the brightest stars in our sample, Mathieu (1983) measured a cluster RV dispersion, after correcting for measurement errors, of $0.48 \pm 0.09 \text{ km s}^{-1}$. After also correcting for undetected binaries (assuming a 50% binary frequency), Mathieu

(1983) find an RV dispersion of $0.25 \pm 0.18 \text{ km s}^{-1}$. Girard et al. (1989) show that this RV dispersion increases to $0.48 \pm 0.15 \text{ km s}^{-1}$ (corrected for both measurement errors and undetected binaries) when including the larger sample from Mathieu et al. (1986), in good agreement with the result we find here.

More recently, Pasquini et al. (2012) derive an RV dispersion for main-sequence stars in M67 with $V < 15$ of $0.680 \pm 0.063 \text{ km s}^{-1}$, and for M67 giants of $0.540 \pm 0.090 \text{ km s}^{-1}$, using HARPS spectra with a typical precision of $\sim 10 \text{ m s}^{-1}$ (not corrected for undetected binaries). If we divide our sample into the SM main-sequence stars with $V < 15$ and SM giant stars, after correcting for measurement errors, we find a combined velocity dispersion for the main-sequence stars of $0.83 \pm 0.04 \text{ km s}^{-1}$ and for giants of $0.60 \pm 0.08 \text{ km s}^{-1}$. However, the main-sequence stars have a much higher binary frequency than the giants, and therefore a much larger correction for undetected binaries. After correcting for both measurement errors and undetected binaries, we find a true velocity dispersion for main-sequence stars ($V < 15$) of $0.60^{+0.08}_{-0.07} \text{ km s}^{-1}$ and for giants of $0.60 \pm 0.10 \text{ km s}^{-1}$. Thus we find essentially identical velocity dispersions for the main-sequence and giant stars. We note that Padova isochrones indicate a mean mass for the main-sequence stars in this sample of $1.11 M_{\odot}$ (with a standard deviation of $0.10 M_{\odot}$), and for the giants of $1.33 M_{\odot}$ (with a standard deviation of $0.01 M_{\odot}$); our sample covers only a narrow mass range.

One-dimensional proper-motion dispersion measurements from the literature are somewhat higher than these RV dispersions (as was also noted by Girard et al. 1989). McNamara & Sanders (1978) find a velocity dispersion of 0.95 km s^{-1} with a 1σ upper limit of $< 1.48 \text{ km s}^{-1}$. Zhao et al. (1996) find a dispersion of $0.96 \pm 0.09 \text{ km s}^{-1}$, and Girard et al. (1989) find a dispersion of $0.81 \pm 0.10 \text{ km s}^{-1}$. As discussed above, the Girard et al. (1989) proper motions have the highest precision, and therefore here we will compare directly to their result. After correcting for undetected binaries, our true RV dispersion measurement differs from the Girard et al. (1989) proper-motion dispersion measurement at about the 2σ level (without accounting for an additional uncertainty on the proper-motion dispersion from the range in cluster distances quoted in the literature). Given the uncertainties on these measurements, the different distances assumed in converting from angular proper motions to km s^{-1} , and the different methods used to account for measurement error in the proper-motion dispersions, we conclude that the RV and proper-motion dispersions are in agreement at our level of precision.

We have also examined the true RV dispersion of M67 as a function of radius from the cluster center, shown in Figure 10. We divide this sample of main-sequence, subgiant and giant single members into five equal bins in radius. Crosses, open circles and filled circles show the observed, combined and true RV dispersion values, respectively, at each bin in radius. The correction for undetected binaries is highest in the inner-most bin, as this bin has the highest binary frequency, consistent with our finding that the binaries are mass segregated with respect to the single stars (see Figure 9).

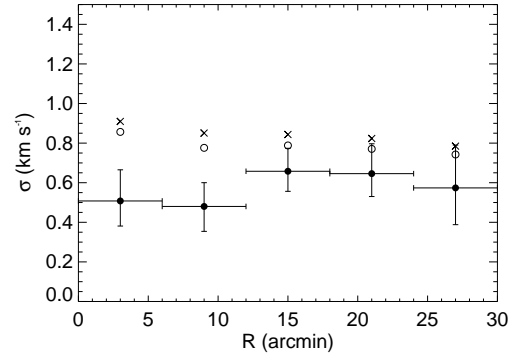


FIG. 10.— Radial-velocity dispersion as a function of radius from the cluster center. Only single main-sequence stars, subgiants and giants with $V \leq 15.5$ are used for this analysis. The observed radial-velocity dispersions are shown with crosses, combined radial-velocity dispersions (after correcting for the contribution from measurement error) are shown in open circles, and the true radial-velocity dispersions (after also correcting for undetected binaries) are shown in filled circles. The horizontal bars show the range in radius of each bin, and the vertical bars show the uncertainties on the velocity dispersion values. All uncertainties are derived as in Geller et al. (2010).

The radial distribution of the true velocity dispersion within the parameter space covered by our survey is consistent with an isothermal distribution. Zhao et al. (1996) find an increase in the proper-motion dispersion as a function of radius, although they note that this effect may be in part due to increased field-star contamination with radius in their sample. We do not see a similar trend in our data. We have also examined different binnings with no detectable effect on the results presented here.

Given the velocity dispersion, we can estimate the mass of the cluster through the virial theorem. Under the assumption that the cluster is in dynamical equilibrium, the kinetic and potential energies are related by $V^2 = \eta GM/R$. From (Spitzer 1987), if this equation is rewritten in terms of the half-mass radius (r_h), $\eta \sim 0.4$ for most systems. Also, for an isotropic velocity dispersion, the observed half-mass radius in projection is given by $r_{hp} \sim \frac{3}{4} r_h$, and the one-dimensional RV dispersion is related to the rms velocity V by $\sigma_r^2 = V^2/3$. Thus the virial mass of the cluster can be calculated by the equation:

$$M_V = 10 \frac{r_{hp} \sigma_r^2}{G}. \quad (2)$$

Fan et al. (1996) find a half-mass radius of M67 for stars with $13.8 < V < 14.5$ of $2.54 \pm 0.41 \text{ pc}$ and for stars with $15.6 < V < 14.5$ of $2.74 \pm 0.29 \text{ pc}$, assuming a distance of 850 pc . The M67 sample used here extends from $V \sim 8$ to $V = 15.5$, though the vast majority of the stars have $V \gtrsim 12.5$. We will assume a projected half-mass radius for the stars in our sample of $r_{hp} = 2.58 \pm 0.45 \text{ pc}$. This value lies in the middle and extends to the limits of the range in r_{hp} found by Fan et al. (1996) for these two magnitude regimes. Given our true RV dispersion above of $\sigma_r = 0.59^{+0.07}_{-0.06} \text{ km s}^{-1}$, we find a virial mass for M67 of $2100^{+610}_{-550} M_{\odot}$.

This value is in good agreement with previous dynamical

ical mass estimates. McNamara & Sanders (1978) derive a virial mass of $1600 M_{\odot}$ (with a 1σ upper limit of $4000 M_{\odot}$), and a direct cluster mass of $1100 M_{\odot}$ based on star counts. Zhao et al. (1996) find a virial mass of $1500 \pm 250 M_{\odot}$ using their proper motions. From examination of the cluster luminosity function, Fan et al. (1996) calculate a mass of $1270 M_{\odot}$ within a radius of 2000 arcsec and including stars with masses $> 0.5 M_{\odot}$.

These mass estimates (including ours) are somewhat higher than the mass estimates of Montgomery et al. (1993), Francic (1989) and Mathieu (1983), who find cluster masses of $724 M_{\odot}$, $553 M_{\odot}$ and $903 M_{\odot}$, respectively, all through analyses of the cluster luminosity function. We interpret these measurements as lower limits on the true cluster mass, as each of these surveys were limited either in magnitude or radial extent.

7. SUMMARY

This is the first in a series of papers studying the dynamical state of the old open cluster M67 through precise RVs. Here we focus on determining cluster membership and identifying binaries (Sections 5) within a complete sample of cluster stars. In total, we present results from 13776 RV measurements of 1278 stars in the direction of M67 spanning from the brightest stars in the cluster down to about 4 magnitudes below the main-sequence turnoff ($V = 16.5$), covering a mass range of about $1.34 M_{\odot}$ to $0.76 M_{\odot}$, and extending spatially to 30 arcmin in radius from the cluster center (about 6 or 7 core radii). We combine RV measurements from multiple telescopes using different instruments, carefully accounting for their different single-measurement RV precisions (see Section 3.1). The vast majority of the stars in our sample have multiple epochs of RV measurements, allowing for the detection of binary companions. For some stars, the time span of our observations exceeds 40 years, and about one third of these stars have observations spanning at least 10 years.

In our analysis, we require at least 3 RV measurements before attempting to determine RV variability or RV membership probabilities. We also utilize the proper-motion membership surveys of Sanders (1977), Girard et al. (1989), Zhao et al. (1993) and Yadav et al. (2008) to remove additional non-members from our cluster sample. Using both proper-motion and RV membership information, we identify 562 cluster members within our sample, 142 of which show significant RV variability, indicative of a binary companion (or multiple companions).

We define a primary sample of stars with $V \leq 15.5$ and within 30 arcmin from the cluster center, where we have ≥ 3 RV measurements for all proper-motion members (and, considering the entire primary sample, at least one RV measurement for all but 1 star and ≥ 3 RV measurements for all but 4 stars; see Section 4.1). We then use this primary sample to construct a CMD cleaned from field-star contamination (Section 6.1), identify and discuss a few notable stars (Section 6.2), compare the projected radial distributions of different cluster populations (Section 6.3), and determine the RV dispersion and virial mass of the cluster (Section 6.4).

Within our cluster member sample, we identify 14 BSS, 4 bright “yellow giants” residing on the CMD between the typical BSS region and the giant sequence (though

one is outside of a 30 arcminute radius from the cluster center), and 2 “sub-subgiants” located to the red of the main-sequence but fainter than the subgiant and giant branches. These “exotic” stars have a remarkably high binary frequency of (at least) 80%, as compared to 22.7% detected binaries amongst the rest of the sample.

Both the binaries and BSS are significantly more centrally concentrated than the single stars (i.e., non-RV variables) in our sample. Within our sample the binaries are, on average, more massive than the single stars, and therefore this result confirms that M67 is mass segregated (as also found by other authors), which is expected for a cluster that has lived through tens of relaxation times. As Mathieu & Latham (1986) also discuss, the central concentration of the BSS suggests that they too are more massive than the single stars in our sample, which is consistent with the predictions of theoretical formation channels. We do not observe a bimodal radial distribution for the BSS, as is observed for BSS in many globular clusters and those in the old open cluster NGC 188. However, our sample only extends to roughly 6 or 7 core radii, and a larger radial extent would likely be required to detect a possible halo BSS population and bimodal radial distribution.

Finally, we determine the RV dispersion of the single main-sequence, subgiant and giant members in our primary sample. Accounting for measurement errors, we find a combined RV dispersion of $0.80 \pm 0.04 \text{ km s}^{-1}$. When also corrected for the contribution from undetected binaries, we find a true RV dispersion of the cluster of $0.59^{+0.07}_{-0.06} \text{ km s}^{-1}$. The radial distribution of the true RV dispersion within our sample is consistent with an isothermal distribution. Using this true RV dispersion and a projected half-mass radius of $r_{\text{HP}} = 2.58 \pm 0.45 \text{ pc}$, we calculate a virial mass for M67 of $2100^{+610}_{-550} M_{\odot}$.

Our long-term RV survey of M67 enables a detailed study of the cluster’s binary population, from the main-sequence through the giant branch and including the rich population of M67 BSS. Future papers in this series will focus on the binary properties of the cluster (e.g., binary frequency and distributions of orbital elements). In particular, we have determined orbital solutions for 108 binary members of the cluster, which we will present and analyze in subsequent papers. Additionally, we will study the binary properties of the BSS in detail, which are critical for our understanding of their formation mechanism(s) (e.g. Geller & Mathieu 2011; Mathieu & Geller 2015). Indeed, binary stars play a primary role in the dynamical evolution of star clusters and the formation of exotic stars like BSS. With the addition of the binary properties to the large body of existing observational work on the cluster, M67 will be invaluable to our theoretical understanding of stellar dynamics, stellar evolution, the formation of BSS, and the long-term evolution of star clusters.

The authors would like to thank the many individuals who helped obtain these spectra and determine the stellar radial velocities, both at the CfA: Jim Peters, Bob Davis, Ed Horine, Perry Berlind, Ale Milone, Robert Stefanik, Mike Calkins, John Geary, Andy Szentgyorgyi, Gabor Furesz, and at the University of Wisconsin - Madison: Natalie Gosnell, Katelyn Milliman, Emily

Leiner, Ben Tofflemire. We would also like to express our gratitude to the staff of the WIYN Observatory for their skillful and dedicated work that have allowed us to obtain these excellent spectra. We thank Imants Platais for his help in cross referencing between the various catalogs in the literature for M67. We also thank any other undergraduate and graduate students not mentioned here explicitly who have contributed late nights

to obtain the spectra for this project. A.M.G. is funded by a National Science Foundation Astronomy and Astrophysics Postdoctoral Fellowship under Award No. AST-1302765. This work was also supported by NSF grant AST 0406615 and the Wisconsin Space Grant Consortium.

Facilities: Tillinghast 1.5m, WIYN 3.5m, MMT, Palomar Hale 5m, Wyeth 1.5m, Haute Provence

REFERENCES

- Andronov, N., Pinsonneault, M. H., & Terndrup, D. M. 2006, *ApJ*, 646, 1160
- Balaguer-Núñez, L., Galadí-Enríquez, D., & Jordi, C. 2007, *A&A*, 470, 585
- Belloni, T., Verbunt, F., & Mathieu, R. D. 1998, *A&A*, 339, 431
- Bevington, P. R., & Robinson, D. K. 1992, *Data reduction and error analysis for the physical sciences*, 2nd edition (New York: McGraw-Hill)
- Bonatto, C., & Bica, E. 2003, *A&A*, 405, 525
- Bruclassi, A., et al. 2014, *A&A*, 561, L9
- Bruntt, H., et al. 2007, *MNRAS*, 378, 1371
- Burstein, D., Faber, S. M., & Gonzalez, J. J. 1986, *AJ*, 91, 1130
- Canto Martins, B. L., Lèbre, A., de Laverny, P., Melo, C. H. F., Do Nascimento, J. D., Jr., Richard, O., & de Medeiros, J. R. 2006, *A&A*, 451, 993
- Carney, B. W., Latham, D. W., Laird, J. B., Grant, C. E., & Morse, J. A. 2001, *AJ*, 122, 3419
- Carraro, G., Chiosi, C., Bressan, A., & Bertelli, G. 1994, *A&AS*, 103, 375
- Castro, M., Do Nascimento, J. D., Jr., Biazzo, K., Meléndez, J., & de Medeiros, J. R. 2011, *A&A*, 526, A17
- Chen, X., & Han, Z. 2004, *MNRAS*, 355, 1182
- Davenport, J. R. A., & Sandquist, E. L. 2010, *ApJ*, 711, 559
- Demarque, P., Green, E. M., & Guenther, D. B. 1992, *AJ*, 103, 151
- Deng, L., Chen, R., Liu, X. S., & Chen, J. S. 1999, *ApJ*, 524, 824
- Eggen, O. J. 1981, *ApJ*, 247, 503
- Fan, X., et al. 1996, *AJ*, 112, 628
- Ferraro, F. R., et al. 2012, *Nature*, 492, 393
- Ferraro, F. R., et al. 1997, *A&A*, 324, 915
- Francic, S. P. 1989, *AJ*, 98, 888
- Friel, E. D., Jacobson, H. R., & Pilachowski, C. A. 2010, *AJ*, 139, 1942
- Geller, A. M., Hurley, J. R., & Mathieu, R. D. 2013, *AJ*, 145, 8
- Geller, A. M., & Mathieu, R. D. 2011, *Nature*, 478, 356
- Geller, A. M., & Mathieu, R. D. 2012, *AJ*, 144, 54
- Geller, A. M., Mathieu, R. D., Braden, E. K., Meibom, S., Platais, I., & Dolan, C. J. 2010, *AJ*, 139, 1383
- Geller, A. M., Mathieu, R. D., Harris, H. C., & McClure, R. D. 2008, *AJ*, 135, 2264
- Giampapa, M. S., Hall, J. C., Radick, R. R., & Baliunas, S. L. 2006, *ApJ*, 651, 444
- Gilliland, R. L., & Brown, T. M. 1992, *AJ*, 103, 1945
- Gilliland, R. L., et al. 1991, *AJ*, 101, 541
- Gilliland, R. L., et al. 1993, *AJ*, 106, 2441
- Girard, T. M., Dinescu, D. I., van Altena, W. F., Platais, I., Monet, D. G., & López, C. E. 2004, *AJ*, 127, 3060
- Girard, T. M., Grundy, W. M., Lopez, C. E., & van Altena, W. F. 1989, *AJ*, 98, 227
- Grocholski, A. J., & Sarajedini, A. 2003, *MNRAS*, 345, 1015
- Hole, K. T., Geller, A. M., Mathieu, R. D., Platais, I., Meibom, S., & Latham, D. W. 2009, *AJ*, 138, 159
- Hurley, J. R., Pols, O. R., Aarseth, S. J., & Tout, C. A. 2005, *MNRAS*, 363, 293
- Hurley, J. R., Tout, C. A., Aarseth, S. J., & Pols, O. R. 2001, *MNRAS*, 323, 630
- Jacobson, H. R., Pilachowski, C. A., & Friel, E. D. 2011, *AJ*, 142, 59
- Janes, K. 1985, in *IAU Symposium*, Vol. 111, *Calibration of Fundamental Stellar Quantities*, ed. D. S. Hayes, L. E. Pasinetti, & A. G. D. Philip, 361
- Janes, K. A., & Smith, G. H. 1984, *AJ*, 89, 487
- Keenan, D. W., Innanen, K. A., & House, F. C. 1973, *AJ*, 78, 173
- Landsman, W., Aparicio, J., Bergeron, P., Di Stefano, R., & Stecher, T. P. 1997, *ApJ*, 481, L93
- Landsman, W., Bohlin, R. C., Neff, S. G., O'Connell, R. W., Roberts, M. S., Smith, A. M., & Stecher, T. P. 1998, *AJ*, 116, 789
- Latham, D. W. 1985, in *Stellar Radial Velocities*, ed. A. G. D. Philip & D. W. Latham, 21
- Latham, D. W. 1992, in *Astronomical Society of the Pacific Conference Series*, Vol. 32, *IAU Colloq. 135: Complementary Approaches to Double and Multiple Star Research*, ed. H. A. McAlister & W. I. Hartkopf, 110
- Latham, D. W. 2007, *Highlights of Astronomy*, 14, 444
- Latham, D. W., & Milone, A. A. E. 1996, in *Astronomical Society of the Pacific Conference Series*, Vol. 90, *The Origins, Evolution, and Destinies of Binary Stars in Clusters*, ed. E. F. Milone & J.-C. Mermilliod, 385
- Leonard, P. J. T. 1996, *ApJ*, 470, 521
- Leonard, P. J. T., & Linnell, A. P. 1992, *AJ*, 103, 1928
- Liu, G. Q., Deng, L., Chávez, M., Bertone, E., Davo, A. H., & Mata-Chávez, M. D. 2008, *MNRAS*, 390, 665
- Loktin, A. V. 2005, *Astronomy Reports*, 49, 693
- Lu, P., Deng, L. C., & Zhang, X. B. 2010, *MNRAS*, 409, 1013
- Manteiga, M., Martinez Roger, C., Morales, C., & Sabau, L. 1991, *A&A*, 251, 49
- Manteiga, M., Martinez Roger, C., & Pickles, A. J. 1989, *A&A*, 210, 66
- Mapelli, M., Sigurdsson, S., Ferraro, F. R., Colpi, M., Possenti, A., & Lanzoni, B. 2006, *MNRAS*, 373, 361
- Marigo, P., Girardi, L., Bressan, A., Groenewegen, M. A. T., Silva, L., & Granato, G. L. 2008, *A&A*, 482, 883
- Mathieu, R. D. 1983, Ph.D. thesis (California Univ., Berkeley.)
- Mathieu, R. D. 2000, in *ASPC*, Vol. 198, "Stellar Clusters and Associations: Convection, Rotation, and Dynamics", ed. R. Pallavicini, G. Micela, & S. Sciortino, 517
- Mathieu, R. D., & Geller, A. M. 2009, *Nature*, 462, 1032
- Mathieu, R. D., & Geller, A. M. 2015, in *Astrophysics and Space Science Library*, Vol. 413, *Ecology of Blue Straggler Stars*, ed. H. M. J. Boffin, G. Carraro, & G. Beccari
- Mathieu, R. D., & Latham, D. W. 1986, *AJ*, 92, 1364
- Mathieu, R. D., Latham, D. W., & Griffin, R. F. 1990, *AJ*, 100, 1859
- Mathieu, R. D., Latham, D. W., Griffin, R. F., & Gunn, J. E. 1986, *AJ*, 92, 1100
- Mathieu, R. D., van den Berg, M., Torres, G., Latham, D., Verbunt, F., & Stassun, K. 2003, *AJ*, 125, 246
- McNamara, B. J., & Sanders, W. L. 1977, *A&A*, 54, 569
- McNamara, B. J., & Sanders, W. L. 1978, *A&A*, 62, 259
- McNamara, B. J., & Sekiguchi, K. 1986, *ApJ*, 310, 613
- Meibom, S., & Mathieu, R. D. 2005, *ApJ*, 620, 970
- Milone, A. A. E. 1992, *PASP*, 104, 1268
- Milone, A. A. E., & Latham, D. W. 1994, *AJ*, 108, 1828
- Montgomery, K. A., Marschall, L. A., & Janes, K. A. 1993, *AJ*, 106, 181
- Murray, C. A., & Clements, E. D. 1968, *Royal Greenwich Observatory Bulletin*, 139, 309
- Nissen, P. E., Twarog, B. A., & Crawford, D. L. 1987, *AJ*, 93, 634
- Önehag, A., Korn, A., Gustafsson, B., Stempels, E., & Vandenberg, D. A. 2011, *A&A*, 528, A85
- Pancino, E., Carrera, R., Rossetti, E., & Gallart, C. 2010, *A&A*, 511, A56
- Pasquini, L., Biazzo, K., Bonifacio, P., Randich, S., & Bedin, L. R. 2008, *A&A*, 489, 677
- Pasquini, L., et al. 2012, *A&A*, 545, A139
- Pasquini, L., Melo, C., Chavero, C., Dravins, D., Ludwig, H.-G., Bonifacio, P., & de La Reza, R. 2011, *A&A*, 526, A127
- Peterson, R. C., Carney, B. W., & Latham, D. W. 1984, *ApJ*, 279, 237

- Piskunov, A. E., Schilbach, E., Kharchenko, N. V., Röser, S., & Scholz, R.-D. 2008, *A&A*, 477, 165
- Pribulla, T., et al. 2008, *MNRAS*, 391, 343
- Qian, S.-B., Liu, L., Soonthornthum, B., Zhu, L.-Y., & He, J.-J. 2006, *AJ*, 131, 3028
- Quinn, S. N., et al. 2014, *ApJ*, 787, 27
- Raghavan, D., et al. 2010, *ApJS*, 190, 1
- Randich, S., Sestito, P., Primas, F., Pallavicini, R., & Pasquini, L. 2006, *A&A*, 450, 557
- Reiners, A., & Giampapa, M. S. 2009, *ApJ*, 707, 852
- Sanders, W. L. 1977, *A&AS*, 27, 89
- Sandquist, E. L. 2004, *MNRAS*, 347, 101
- Sandquist, E. L. 2005, *ApJ*, 635, L73
- Sandquist, E. L., Latham, D. W., Shetrone, M. D., & Milone, A. A. E. 2003, *AJ*, 125, 810
- Sandquist, E. L., & Shetrone, M. D. 2003a, *AJ*, 126, 2954
- Sandquist, E. L., & Shetrone, M. D. 2003b, *AJ*, 125, 2173
- Sarajedini, A., Dotter, A., & Kirkpatrick, A. 2009, *ApJ*, 698, 1872
- Sarajedini, A., von Hippel, T., Kozhurina-Platais, V., & Demarque, P. 1999, *AJ*, 118, 2894
- Shetrone, M. D., & Sandquist, E. L. 2000, *AJ*, 120, 1913
- Spitzer, L. 1987, *Dynamical evolution of globular clusters* (Princeton, NJ, Princeton University Press)
- Stassun, K. G., van den Berg, M., Mathieu, R. D., & Verbunt, F. 2002, *A&A*, 382, 899
- Stefanik, R. P., Latham, D. W., & Torres, G. 1999, in *Astronomical Society of the Pacific Conference Series*, Vol. 185, IAU Colloq. 170: *Precise Stellar Radial Velocities*, ed. J. B. Hearnshaw & C. D. Scarfe, 354
- Stello, D., et al. 2007, *MNRAS*, 377, 584
- Taylor, B. J. 2007, *AJ*, 133, 370
- Tian, B., Deng, L., Han, Z., & Zhang, X. B. 2006, *A&A*, 455, 247
- van den Berg, M., Orosz, J., Verbunt, F., & Stassun, K. 2001, *A&A*, 375, 375
- van den Berg, M., Stassun, K. G., Verbunt, F., & Mathieu, R. D. 2002, *A&A*, 382, 888
- VandenBerg, D. A., & Stetson, P. B. 2004, *PASP*, 116, 997
- Vasilevskis, S., Klemola, A., & Preston, G. 1958, *AJ*, 63, 387
- Yadav, R. K. S., et al. 2008, *A&A*, 484, 609
- Yakut, K., et al. 2009, *A&A*, 503, 165
- Zhang, X. B., Zhang, R. X., & Deng, L. 2005, *AJ*, 129, 979
- Zhao, J. L., Tian, K. P., Pan, R. S., He, Y. P., & Shi, H. M. 1993, *A&AS*, 100, 243
- Zhao, J. L., Tian, K. P., & Su, C. G. 1996, *Ap&SS*, 235, 93

TABLE 4
RADIAL-VELOCITY DATA TABLE

ID_W	ID_X	RA	Dec	V	$(B-V)$	N_W	N_C	JD_0	JD_f	\overline{RV}	RV_e	i	P_{RV}	P_{PM_y}	P_{PM_z}	P_{PM_g}	P_{PM_s}	e/i	$P(\chi^2)$	Class	Comment
1001	S1024	8:51:22.91	11:48:49.4	12.720	0.550	0	34	45784.84	47519.82	33.32	0.17	...	98	99	...	99	92	BM	SB2,CX111,PV
2001	S1027	8:51:24.95	11:49:00.8	13.240	0.600	14	13	46808.93	56707.92	32.09	0.15	0.67	93	100	93	99	95	1.18	0.000	SM	X46
3001	S1031	8:51:22.96	11:49:13.1	13.260	0.460	2	32	46808.96	54423.99	33.46	0.30	0.91	98	100	94	99	91	7.76	0.000	BM	SB1
4001	S1029	8:51:21.62	11:49:02.5	15.210	0.790	17	7	47580.74	56705.91	32.60	0.26	0.79	97	97	...	72	83	11.62	0.000	BM	SB1,PV
5001	M5754	8:51:23.50	11:49:05.8	16.220	1.000	3	0	56054.68	56669.01	34.24	0.27	0.74	98	96	0.63	0.669	SM	...
1002	S1023	8:51:26.84	11:48:40.5	10.540	0.570	0	7	41072.69	50822.92	3.92	0.38	0.49	0	84	0	7	0	2.04	0.000	SN	...
2002	S1040	8:51:23.77	11:49:49.3	11.520	0.870	1	57	41073.67	54164.75	33.01	0.08	0.56	98	97	...	99	95	10.05	0.000	BM	SB1,X10,CX6,PV,YG
3002	S1018	8:51:24.09	11:48:21.9	12.830	0.570	0	32	46874.69	48291.90	33.38	0.16	...	98	100	96	99	89	BM	SB2
4002	S1030	8:51:25.95	11:49:08.9	13.230	0.570	2	5	46808.94	56051.71	34.22	0.22	0.77	98	100	...	98	90	0.76	0.653	SM	...
5002	S1032	8:51:26.52	11:49:20.3	13.480	0.570	2	4	47489.97	55934.05	34.24	0.35	0.75	98	100	...	98	96	1.15	0.169	SM	PV

The contents of each column are defined in Section 5.